GnRH replacement rescues cognition in Down syndrome

Maria Manfredi-Lozano, Valerie Leysen, Michela Adamo, Isabel Paiva, Renaud Rovera, Jean-Michel Pignat, Fatima Ezzahra Timzoura, Michael Candlish, Sabiha Eddarkaoui, Samuel Malone, et al.

Published in final edited form as:
Science. 2022 September 02; 377(6610): eabq4515. doi:10.1126/science.abq4515.

GnRH replacement rescues cognition in Down Syndrome

Maria Manfredi-Lozano[1,2,#], **Valerie Leysen**[1,2,#], **Michela Adamo**[3,4,#], **Isabel Paiva**[5], **Renaud Rovera**[6], **Jean-Michel Pignat**[7], **Fatima Ezzahra Timzoura**[1,2], **Michael Candlish**[8,†], **Sabiha Eddarkaoui**[1], **Samuel A. Malone**[1,2], **Mauro S. B. Silva**[1,2], **Sara Trova**[1,2], **Monica Imbernon**[1,2], **Laurine Decoster**[1,2], **Ludovica Cotellessa**[1,2], **Manuel Tena-Sempere**[9], **Marc Claret**[10], **Ariane Paoloni-Giacobino**[11], **Damien Plassard**[12], **Emmanuelle Paccou**[3], **Nathalie Vionnet**[3], **James Acierno**[3], **Aleksandra Maleska Maceski**[13], **Antoine Lutti**[14], **Frank Pfrieger**[15], **S. Rasika**[1,2], **Federico Santoni**[4], **Ulrich Boehm**[8], **Philippe Ciofi**[16], **Luc Buée**[1], **Nasser Haddjeri**[6], **Anne-Laurence Boutillier**[5], **Jens Kuhle**[13], **Andrea Messina**[3,4], **Bogdan Draganski**[14,17], **Paolo Giacobini**[1,2,ξ], **Nelly Pitteloud**[3,4,*,ξ], **Vincent Prevot**[1,2,*,ξ]

[1]Univ. Lille, Inserm, CHU Lille, Lille Neuroscience & Cognition, UMR-S 1172, LabexDistAlz, Lille, France

[2]Laboratory of Development and Plasticity of the Neuroendocrine Brain, FHU 1000 days for health, EGID, Lille, France

[3]Department of Endocrinology, Diabetology, and Metabolism, Lausanne University Hospital, 1011 Lausanne, Switzerland

[4]Faculty of Biology and Medicine, University of Lausanne, Lausanne 1005, Switzerland

[5]Laboratoire de Neurosciences Cognitives et Adaptatives (LNCA), UMR 7364, Université de Strasbourg-CNRS, Strasbourg, France

[6]Univ. Lyon, Université Claude Bernard Lyon 1, Inserm, Stem Cell and Brain Research Institute U1208, Bron 69500, France

[7]Department of Clinical Neurosciences, Neurorehabilitation Unit, University Hospital CHUV, Lausanne, Switzerland

[*]Correspondence to: Nelly.Pitteloud@chuv.ch and vincent.prevot@inserm.fr (+33 612903876).
[†]New address, Institute of Cell Biology and Neuroscience and Buchmann Institute for Molecular Life Sciences (BMLS), University of Frankfurt, Max-von-Laue-Str. 15, 60438, Frankfurt am Main, Germany
[#]These authors contributed equally to this work.
[ξ]These authors contributed equally to this work.

Author contributions: V.P. designed the preclinical study, analyzed data, prepared the figures, and wrote the manuscript along with U.B. and N.P., M.C. and N.P. M.M.-L and V.L. designed and performed the experiments in mice and were involved in all aspects of study design, interpretation of results, manuscript preparation and prepared the figures. N.P. designed the clinical study, M.A. and E.P. performed the clinical study, M.A. analyzed the data, prepared the figures, and wrote the manuscript; N.V. and F.S. contributed to the data analysis and manuscript preparation. A.P-G. contributed to the recruitment of the subjects for the clinical study; B.D. analyzed structural MRI data; and JM.P analyzed the functional MRI data. A.L. contributed to MRI data acquisition using prospective motion correction. S.R. and J.A. contributed to the preparation of the manuscript. A.M.M. and J.K. performed and analyzed the neurofilament light chain analyses. N.H. and R.R. designed and performed in vivo electrophysiology experiments. S.E., F.E.T. and M.I. performed the western blot analyses; I.P., D.P. and A.L.B. performed transcriptomic analyses; M.S.B.S performed the viral tracing injections; S.T. performed GnRHR image analyses; S.A.M. performed tissue-clearing experiments and analyzed the data; L.D., L.C., F.E.T. and P.G. conducted the fluorescent *in situ* hybridization analyses; M.T.-S., U.B, L.B., M.C., M.Cl. and F.P. contributed material; and A.M., L.B., U.B., P.C., N.P., P.G. were involved in the study design, interpretation of the results, and preparation of the manuscript.

Competing interests: M.M.-L., V.L., A.M. P.G. and V.P. disclose that they are inventors of a patent covering the treatment of cognitive disorder and dementia with pulsatile GnRH (82). All other authors do not have competing interests.

Europe PMC Funders Author Manuscripts

[8]Experimental Pharmacology, Center for Molecular Signaling (PZMS), Saarland University School of Medicine, 66421, Homburg, Germany

[9]Univ. Cordoba, IMIBC/HURS, CIBER Fisiopatología de la Obesidad y Nutrición, Instituto de Salud Carlos III, Cordoba, Spain

[10]Neuronal Control of Metabolism Laboratory, Institut d'Investigacions Biomèdiques August Pi i Sunyer (IDIBAPS), 08036 Barcelona, Spain; Centro de Investigación Biomédica en Red (CIBER) de Diabetes y Enfermedades Metabólicas Asociadas (CIBERDEM), 08036 Barcelona, Spain

[11]Department of Genetic Medicine, University Hospitals of Geneva, 4 rue Gabrielle-Perret-Gentil, 1211, Genève 14, Switzerland

[12]CNRS UMR 7104, INSERM U1258, GenomEast Platform, Institut de Génétique et de Biologie Moléculaire et Cellulaire (IGBMC), Université de Strasbourg, Illkirch, France

[13]Neurologic Clinic and Polyclinic, MS Centre and Research Centre for Clinical Neuroimmunology and Neuroscience Basel; University Hospital Basel, University of Basel, Basel Switzerland

[14]Laboratory for Research in Neuroimaging LREN, Centre for Research in Neurosciences, Department of Clinical Neurosciences, Lausanne University Hospital and University of Lausanne, Switzerland

[15]Centre National de la Recherche Scientifique, Université de Strasbourg, Institut des Neurosciences Cellulaires et Intégratives, 67000 Strasbourg, France

[16]Univ. Bordeaux, Inserm, U1215, Neurocentre Magendie, Bordeaux, France

[17]Neurology Department, Max-Planck-Institute for Human Cognitive and Brain Sciences, Leipzig, Germany

Europe PMC Funders Author Manuscripts

Abstract

Currently, no viable treatment exists for cognitive and olfactory deficits in Down syndrome (DS). We show in a DS model (Ts65Dn mice) that these progressive non-reproductive neurological symptoms closely parallel a post-pubertal decrease in hypothalamic as well as extra-hypothalamic expression of a master molecule controlling reproduction – gonadotropin-releasing hormone (GnRH), and appear related to an imbalance in a microRNA-gene network known to regulate GnRH neuron maturation together with altered hippocampal synaptic transmission. Epigenetic, cellular, chemogenetic and pharmacological interventions that restore physiological GnRH levels abolish olfactory and cognitive defects in Ts65Dn mice, while pulsatile GnRH therapy improves cognition and brain connectivity in adult DS patients. GnRH thus plays a crucial role in olfaction and cognition, and pulsatile GnRH therapy holds promise to improve cognitive deficits in DS.

Keywords

Trisomy; dementia; intellectual disability; cognitive decline; preoptic area; hypothalamic-pituitary-gonadal axis; anosmia; infertility; microRNA; Otx2

Introduction

Down syndrome (DS) or Trisomy 21 is the most common genetic cause of intellectual disability, for which treatment options are few and of doubtful efficacy (1, 2). The extra chromosome 21 is associated with increased gene dosage and global alterations of gene expression, disrupting biological homeostasis and contributing to its various clinical and neurological manifestations (3) (4). Among these, adult DS patients present with cognitive decline due to an early-onset Alzheimer disease (AD)-like pathology (5–11), and have also revealed white matter pathology and hypomyelination (12). A progressive loss of olfaction, typical of neurodegenerative diseases, is also prevalent (13), starting during the prepubertal period (14), and men with DS may display deficits in sexual maturation (15).

The inability to perceive odors, together with infertility, is also characteristic of gonadotropinreleasing hormone (GnRH) deficiency in patients with Kallmann syndrome (16). GnRH, essential for reproduction in all mammals (17), is secreted by specialized neurons in the hypothalamus and activates the hypothalamic-pituitary-gonadal (HPG) axis to produce sex steroids (16). However, the first centrally driven gonad-independent activation of the HPG axis occurs well before puberty, during the infantile period in both humans and mice (18, 19), a phenomenon known as “minipuberty” that sets in motion the entire process of reproductive maturation (20). Additionally, the expression of GnRH and its cognate receptor GnRHR in extrahypothalamic areas not directly involved in reproduction suggests a role for GnRH in higher brain functions (21–23). In light of these phenotypic and temporal correlations, we used Ts65Dn mice, which overexpress the mouse genomic region orthologous to chromosome 21 (chromosome 16) (24) and recapitulate many of the anatomical, neurobiological, and behavioral phenotypes of human DS (25–27), to examine whether olfactory and cognitive deficits in DS could stem from GnRH abnormalities, and could be reversed by its replacement in mice and DS patients.

Results

Ts65Dn mice show Down-like olfactory, cognitive deficits

To explore whether olfactory and cognitive deficits, observed in DS patients, also occurred in Ts65Dn mice and determine their temporality, we performed habituation/dishabituation tests to assess odor discrimination (28), and a novel object recognition test (also used in DS patients (29)) to assess recognition memory, a hippocampus-dependent task (30), in prepubertal (P35) and young adult (P90) mice (Fig. 1A). While olfactory performance in Ts65Dn mice was normal at birth (as assessed by milk intake, an olfaction-dependent behavior in newborns) and the infantile period (assessed using the homing test) (Fig. S1), olfactory deficits appeared between the second week of life and the juvenile period. While male and female prepubertal (P35) Ts65Dn mice showed normal habituation (i.e. reduced sniffing time when an odor was reintroduced), once habituated, they were unable to distinguish novel from known odors (Fig. 1B), a deficit that persisted in adulthood (Fig. 1C), phenocopying the prepubertal onset of olfactory deficits in DS patients (14). In contrast, novel object recognition in prepubertal Ts65Dn mice was comparable to wild-type (WT) littermates (Fig. 1D) but impaired in young adults (Fig. 1E), revealing an age-dependent cognitive decline reminiscent of DS. Two alternative explanations for age-related cognitive

deterioration - neuroinflammation (31) and triplication of the amyloid precursor protein (*App*) gene in both DS patients and Ts65Dn mice (24) – were eliminated, as inflammatory markers were comparable between the two genotypes (Fig. S2), and any changes in the expression of AD-related proteins occurred in middle-aged (P360) but not young adult (P90) Ts65Dn animals (Fig. S3), i.e. well after the onset of olfactory and cognitive changes.

With regard to sexual development and reproductive maturation, Ts65Dn mice are known to show abnormalities (24), with males being infertile and females subfertile (32). We found, additionally, that males displayed severe hypogonadism in adulthood (Fig. S4), whereas females showed normal puberty timing and regular estrous cyclicity as young adults, but became anovulatory at 12 months of age (Fig. S5). These sexually dimorphic phenotypes also resemble those reported in DS patients (15). To understand whether these changes stemmed from alterations to the HPG axis, we measured serum gonadotropin levels. Adult male (Fig. 2A-C) and female (Fig. S5I-K) Ts65Dn mice showed normal luteinizing hormone (LH) pulse frequency but decreased LH pulse amplitude. However, at P12, during the peak of minipuberty, levels of the gonadotropins LH and follicle stimulating hormone (FSH) were not markedly altered in female Ts65Dn mice (Fig. S5L). In male Ts65Dn mice at P12, LH but not FSH levels were higher than in WT mice, while both gonadotropins were elevated in adulthood (Fig. 2D), a phenomenon also seen in DS men (15, 33). Despite this, adult male Ts65Dn mice displayed unaltered testosterone levels (Fig. 2D), similar to DS men (15). However, serum LH levels before, and 14 and 30 days after bilateral orchidectomy were comparably increased in both groups (Fig. 2E), indicating intact gonadal steroid communication between the testes and the hypothalamus. Similarly, orchidectomy did not affect olfactory or cognitive performance (Fig. 1F,G), suggesting that any deficits were not due to gonadal steroid deficiency or altered gonad-brain communication.

Together, these results confirm that trisomic Ts65Dn mice also reproduce the olfactory, cognitive and sexually dimorphic reproductive phenotype of DS patients, and implicate HPG axis dysregulation as a putative cause of these deficits.

GnRH is progressively lost in Ts65Dn mice

In keeping with our studies in human fetuses (21), three-dimensional (3D) imaging and analyses of solvent-cleared tissue (iDISCO) from adult WT mice revealed numerous extra-hypothalamic GnRH projections (Fig. 2F), often in close apposition to the walls of the lateral ventricles (Movie S1-2). Unilateral stereotaxic injections of adeno-associated viral vectors encoding Yellow Fluorescent Protein (AAV9.EF1a.DIO.eYFP.WPRE.hGH) into the dorsolateral median eminence, where GnRH neuroendocrine terminals are located, in adult WT *Gnrh*::*Cre* mice (Fig. S6A) led to YFP labeling not only of GnRH neuronal cell bodies and processes in the preoptic area (POA) (Fig. S6B,C), but also of processes in the cortex (Fig. S6D,E), hippocampus (Fig. S6D,F) and paraventricular thalamus (Fig. S6D,F). Thus, at least some extra-hypothalamic GnRH projections in brain areas controlling cognitive and social behaviors actually came from hypophysiotropic GnRH neurons in the hypothalamus (Fig. 2F, S6A). iDISCO analyses of *Gnrhr*::*Cre;Tau-GFP*$^{loxp/+}$ mice also identified GFP-labeled neurons expressing the GnRH receptor (GnRHR) promoter in the mouse cerebral cortex and hippocampus (Fig. 2G, S7A-F), supporting a non-reproductive role for GnRH.

Using conventional immunohistofluorescence and iDISCO, which provide comparable and accurate counts of GnRH neurons (21, 34), we found no difference in either the distribution or the number of GnRH somata at birth (P0) between Ts65Dn and WT mice regardless of sex, but a profound loss of both hypothalamic and extra-hypothalamic GnRH-immunoreactive somata and fibers starting after puberty onset in Ts65Dn mice (Fig. 2H, Fig. S8). In adult (P90) Ts65Dn mice, although GnRH fibers were visible in the median eminence (Fig. 2I), extensive extra-hypothalamic GnRH projections were absent (Fig. 2F,I), mirroring the age-related deterioration of cognitive performance observed in these mice (Fig. 1D,E).

microRNA-transcription factor imbalances underlie olfactory, cognitive impairments

HPG axis activation through GnRH expression at minipuberty (P12) is regulated by a complex switch consisting of several microRNAs—in particular miR-155 and the miR-200 family, as well as their target transcriptional repressor/activator genes, in particular *Zeb1* and *Cebpb* (Fig. 3A) (18). Human chromosome 21 and murine chromosome 16 code for at least five of these microRNAs (miR-99a, let-7c, miR-125b-2, miR-802 and miR-155), of which all except miR-802 are selectively enriched in GnRH neurons in WT mice around minipuberty (18). Given the peripubertal loss of GnRH-immunoreactivity in Ts65Dn mice, we analyzed global microRNA and gene expression in the POA in adult mice and found a downregulation of miR99a, as well as smaller decreases in let-7c, miR-125b-2, miR-802 and miR-155 (Fig. 3B). Despite not being located on chromosome 16, miR-200 family members were reduced by 50% or more (Fig. 3C), accompanied by an upregulation of *Zeb1* mRNA and a consequent marked decrease in *Gnrh1* expression (Fig. 3D). Real-time PCR analyses of cell-sorted GnRH neurons from *Gnrh*::*gfp*;Ts65Dn mice (Fig. S9; Fig. 3E) confirmed that this increase in *Zeb1*, a *Gnrh1* promoter repressor, and a concomitant downregulation of the *Gnrh1* promoter activators *Otx2* and *Kiss1r* already occurred during the infantile period, i.e. minipuberty (Fig. 3F), initiating decreased *Gnrh1* expression (Fig. 3D). Accordingly, the selective overexpression of miR-200b in the POA of adult (P90) Ts65Dn males using stereotaxic injections of AAV9-EF1a-mmu-mir200b-eGFP but not a control vector (Fig. 3G,H; Fig. S10A,B), which rescued the capacity to differentiate odors (Fig. 3L) and recognize novel objects (Fig. 3M), also increased the number of neurons expressing *Gnrh1* (Fig. 3I-K, Fig. S10D) and the *Gnrh1* promoter regulator *Otx2* (Fig. S10C,D, Fig. 3I) in the POA. Conversely, male *Gnrh::Cre;Dicer*$^{loxP/loxP}$ mice, in which miRNA processing (and thus GnRH expression) is selectively knocked out in GnRH neurons, phenocopied Ts65Dn mice, displaying impaired olfactory discrimination and cognition (Fig. 3N,O).

Hypothalamic miR-200b overexpression rectifies hippocampal gene expression

To further analyze how miR-200 expression in the POA could influence cognitive function, we performed RNA-seq and differential gene expression analyses of the POA and hippocampus dissected from 6-8 month-old WT and Ts65Dn littermates injected in the POA with control AAV, and from Ts65Dn mice infected with the vector overexpressing miR-200b (Fig. S11A). While 8 genes were differentially expressed in the POA of Ts65Dn vs. WT littermates (Fig. S11B), 91 were differentially expressed in the hippocampus (Fig. 4A-B), many involved in axon ensheathment, myelination and oligodendrocyte differentiation, as well as in potassium ion transport (Fig. 4C), in agreement with previous

transcriptomic studies of the hippocampus of autopsied DS patients and mouse models (35) (12). Downregulated genes were involved in G-protein-coupled receptor signaling, amino acid transport and neurotransmission (Fig. S11C-D).miR-200b overexpression for 3 months in the POA of adult Ts65Dn mice reversed the upregulation of 53 of 72 genes in the hippocampus (Fig. 4D), in particular those involved in the aforementioned biological processes (Fig. S11E), and the downregulation of 6 of 19 genes (Fig. S11D). This phenomenon was confirmed by qRT-PCR analyses for key genes involved in axon ensheathment, myelination and oligodendrocyte differentiation, including myelin basic protein (*Mbp*) and inhibitor of DNA binding 4 (*Id4*), and potassium ion transport, such as the potassium channel *Kcnj13* and aquaporin 1 (*Aqp1*) (Fig. 4E, Fig. S11F,G). Additionally, 7 genes upregulated in the Ts65Dn hippocampus are known to be similarly altered in DS patients (Fig. S12A) (35), and include 4 that are involved in myelination, of which the upregulation of 3 is reversed by miR-200b overexpression in the POA of Ts65Dn mice (Fig. S12B). However, while protein levels of two of these, Kcnj13 and Mbp, in the contralateral hippocampus of the same animals showed an effect of miR-200b, there were discrepancies in the direction of change between the two analyses, as might be expected given the complex control mechanisms involved, and the concomitant up- or downregulation of other transcriptional regulators, such as the known Mbp transcriptional stabilizer Quaking (Qk) (36) (Fig S11F,G), which can also act as translational repressor depending on the molecular context (37, 38). Similarly, transcripts for the multifunctional homeoprotein *Otx2* (39) were upregulated in the hippocampal Cornu Ammonis area 1 (CA1) in Ts65Dn mice, in contrast to the POA (Fig. S10C,B), but normalized by preoptic miR-200b overexpression (Fig. S12C-E). Regardless of the direction of these changes, they provide a putative molecular basis for anomalies of brain structure and composition in DS patients (12), and their reversal by miR-200b infusion in the POA is of both mechanistic and therapeutic interest.

Hypothalamic miR-200b overexpression rectifies hippocampal synaptic transmission

Next, to explore whether the functional basis of recognition memory was altered in Ts65Dn mice, we assessed basal hippocampal synaptic transmission *in vivo* by stimulating commissural fibers from the left hippocampus in anesthetized mice, and for each stimulation site, recording both population spikes and field excitatory post-synaptic potentials (fEPSPs) from CA1 stratum radiatum of the contralateral hippocampus (Fig. 4F). Paired-pulse stimulation (Fig. S13A) revealed similar facilitation of fEPSPs in the CA1 pyramidal cell layer of WT and Ts65Dn mice (Fig. S13B). However, the stimulus-response curve obtained by recording both fEPSPs and population spikes in the CA1 (Fig. 4G, Fig. S13C) as well as the area under the curve (Fig. 4H), were significantly lowered in Ts65Dn compared to WT mice, suggesting lower dendritic excitability. These changes were diminished by miR-200b overexpression in the POA (Fig. 4G,H, Fig. S13D). To further examine the relationship between synaptic input strength and the amplitude and latency to firing of CA1 pyramidal cells, we analyzed population spike-fEPSP coupling at different stimulation intensities (Fig. 4I). The highest and lowest values on the Boltzmann-fitted population spike-fEPSP curve were lower in Ts65Dn mice than in WT animals, reflecting a lower maximal-minimal spike amplitude in Ts65Dn mice that was rescued by miR-200b overexpression (Fig. 4J). While latency did not significantly change (Fig. 4K, Fig. S13 E, F), cellular excitability was lowered in Ts65Dn mice and partially reversed by miR-200 overexpression (Fig. 4L).

Together, these results suggest that miR-200 family expression in the POA alters electrical signal propagation in the hippocampus, and that these deficits can be remotely rescued by overexpressing miR-200b in the hypothalamus.

Hypothalamic GnRH compensation reverses olfactory and cognitive deficits

We next attempted to rescue olfactory and cognitive function in adult Ts65Dn mice by GnRH replacement. Stereotactic injection of dissociated cells (18) from the POA of neonatal WT *Gnrh::gfp* pups (WT-POA) into the third ventricle (3V) of adult male and female Ts65Dn mice (Fig. 5A, Fig. S14) (40) completely reversed both olfactory and cognitive impairments in Ts65Dn males (Fig. 5B) as well as short-term visuospatial memory assessed in a Y-maze test (Fig. 5C-E). Graft of WT-POA also rescued cognition in adult Ts65Dn females, but only partly restored olfactory capacity (Fig. 5F). However, unlike adult hypogonadal mice (40), WT-POA transplantation did not restore fertility in either Ts65Dn females (Fig. S15) or males (see methods). We next generated *Gnrh::Cre*; *BoNTB*$^{\text{loxP-STOP-loxP}}$ mice in which vesicular GnRH release is selectively silenced by the GnRH-neuron-specific expression of botulinum neurotoxin B (*BoNTB*$^{\text{Gnrh}}$). When neonatal POA cells from these animals were grafted into adult Ts65Dn males (Fig. 5G), no olfactory or cognitive rescue was observed (Fig. 5H,I). However, intraperitoneal GnRH injection 6 months post-graft rescued olfactory and cognitive performance in both sham (Fig. 5B) and *BoNTB*$^{\text{Gnrh}}$ POA-grafted Ts65Dn mice (Fig.5H,I), indicating that the effects of the graft were specifically due to GnRH release.

To determine whether activating endogenous GnRH neuronal activity in Ts65Dn mice could rescue olfactory and cognitive function, we bilaterally injected adult *Gnrh::Cre* and Ts65Dn;*Gnrh::Cre* mice with a Cre-dependent neuron-activating hM3Dq-DREADD (Designer Receptor Exclusively Activated by Designer Drugs) vector into the POA (Fig. 5J). Unlike vehicle injection (Fig. 5K,M), intraperitoneal clozapine N-oxide (CNO) injections elicited increased LH levels in both *Gnrh::Cre* and Ts65Dn;*Gnrh::Cre* males (Fig. 5L,N), indicating GnRH release. Additionally, they acutely restored olfactory discrimination (Fig. 5O) and cognitive performance (Fig. 5P) in Ts65Dn mice. Conversely, when neurons expressing GnRHR in the hippocampus of WT *Gnrhr::Cre* mice were infected with an inhibitory DREADD vector (AAV8-hSYN-DIO-hM4D(Gi)-mCherry) (Fig. 5Q), acute CNO injection (3 mg/kg) dramatically reduced both cognitive and olfactory performance (Fig. 5R,S).

These data together highlight the possibility that normal cognitive and olfactory function depends on extra-hypothalamic GnRH neuronal projections and action, which are lost in Ts65Dn mice during postnatal development, leading to their DS-like phenotype.

GnRH pulsatility is essential for deficit reversal

Finally, we tested whether restoring physiological (i.e. pulsatile) GnRH release in Ts65Dn mice could reverse cognitive performance using Lutrelef - the native GnRH used to treat hypogonadotropic infertility (41, 42). Adult Ts65Dn males were implanted with a subcutaneous programmable mini-pump that delivered either pulsatile Lutrelef (0.25 μg of GnRH per pulse over 10 min given every 3h), leading to activation of the GnRH

receptor and the reproductive axis, or continuous Lutrelef infusion (0.25 μg per 3h), which downregulates the GnRH receptor and blocks the reproductive axis (43), for 15 days (Fig. 6A). Continuous infusion did not improve olfactory or cognitive performance in male Ts65Dn mice, and had a significant deleterious effect in WT mice (Fig. 6B,C), in addition to blunting LH pulsatility (Fig. 6D-I). In contrast, pulsatile Lutrelef, which rescued both olfactory discrimination (Fig. 6B) and cognitive function (Fig. 6C), increased LH pulse amplitude to WT levels in Ts65Dn males (Fig. 6D). Neither Lutrelef treatment nor miR-200b overexpression in the POA rescued testicular weight in Ts65Dn mice (Fig. S16). Bilateral orchidectomy did not affect the rescue of olfaction (Fig. 6J) or recognition memory (Fig. 6K) by pulsatile Lutrelef, suggesting that the functional improvements observed were independent of the gonadotropic effects of GnRH, and could instead be due to the mobilization of cognitive reserves in Ts65Dn mice.

Pulsatile GnRH improves cognition in Down Syndrome patients

Based on compelling results in Ts65Dn mice, we conducted an open-label pilot study to assess the effects of pulsatile GnRH therapy on cognition in DS patients. Seven DS men (26.4±2.3 years) who had completed puberty and presented with olfactory defects were enrolled (Table S1). Despite normal testosterone and inhibin B levels, patients exhibited mildly elevated LH and FSH levels, and a mild increase in estradiol levels as compared to controls (Fig. 7A-D, Fig. S17C), yet normal pituitary sensitivity to a GnRH challenge (Fig. S17A-B). LH pulsatility was not assessed in this vulnerable population. DS patients displayed normal BMI and no major alteration in biochemical profile except for increased hsCRP, i.e., systemic inflammation (Fig. 7F, Table S1). Serum neurofilament light chain, a marker of neuronal damage (44), was within the normal range for age (Fig. S17S). The Montreal Cognitive Assessment (MoCA) score was used to assess cognition in DS patients for whom long cognitive battery tests are challenging, given their intellectual disability, attention deficit and fatigue. The seven DS patients had impaired cognition (Fig. 7G-K), while 4 had altered verbal comprehension (Token test) (Fig. 7L). Using quantitative relaxometry-based MRI, we observed DS-related loss of myelin along the corticospinal tract and thalamus, increased iron in the pallidum, and volume loss in the cingulate gyrus, cerebellum and thalamus, compared to healthy age-matched controls (Fig. 7N, Fig. S17R, Table S2-3) (45). Resting-state functional magnetic resonance imaging (rs-fMRI) showed altered default mode network (DMN) in our DS cohort (Fig. 7O), as previously reported (46, 47).

Pulsatile GnRH therapy using a LutrePulse pump was given for 6 months at a dose of 75ng/kg/pulse every two hours to mimic the LH pulse frequency observed in healthy men (41), and was well tolerated (Fig. S17L-M). The reproductive hormonal profile did not change on GnRH therapy (Fig.7A-C, S17A, Table S1) except for a slight decrease in serum FSH (Fig.7D). Most metabolic parameters showed a trend towards improvement or no change (Fig. S17D-K,S, Table S1). Cognitive performance, as assessed by total MoCA score, increased in 6 out of 7 patients (Fig. 7G), driven by sub-scores for visuospatial function (Fig. 7H,M), executive function (Fig. 7I), attention (Fig. 7J) and a trend for episodic memory (Fig. 7K). GnRH therapy also enhanced verbal comprehension (Fig. 7L). Olfactory performances (Fig. S17N-Q) and brain anatomical features did not change

(Tables S2-S3, Fig. S18A-D). However, functional connectivity as assessed by rs-fMRI increased mainly within a broad network encompassing visual and sensorimotor DMN regions, while connectivity within the hippocampal regions (ventral DMN) linked to the amygdala decreased (Fig. 7O), approaching control values (46, 48, 49).

Discussion

Our study demonstrates an unexpected role for GnRH in olfactory and cognitive performance, consistent with the expression of GnRH and its cognate receptor GnRHR in extra-hypothalamic areas (21–23). The progressive loss of GnRH expression during postnatal development precedes the onset of cognitive and olfactory impairments in a mouse model of DS, which can be reversed by replacing GnRH. Furthermore, in our pilot study of DS patients pulsatile GnRH therapy improved cognition, consistent with improved connectivity in the relevant brain regions. This is particularly important given that translational studies in DS have fallen short, and no pharmacological therapy to date has significantly improved cognition (1, 50–53).

In DS patients, a deviation from neurotypical developmental trajectories leads to reduced cognitive abilities (54) and AD-like neurodegenerative changes in their forties after a long preclinical phase (5, 6, 11, 55). Olfactory deficits of prepubertal onset worsen in adulthood concomitant with the acceleration of cognitive decline (14). In our trisomic model, which faithfully phenocopies several clinical aspects of DS, cognitive and olfactory deficits parallel a gradual loss in GnRH expression beginning in childhood and culminating in adulthood, well before any AD-like changes. The loss of GnRH itself can be traced even further back, to the perturbation of the minipubertal microRNA-transcription factor switch in *Gnrh1* promoter activity during the infantile period, which integrates multiple feedback loops (18), and is partially localized on the triplicated region of both the human and mouse chromosome. Overexpressing miR-200b, one of the effectors of this switch, in the hypothalamic POA, where most GnRH neuronal cell bodies reside, not only rescues other genes of the GnRH transcriptional regulation network but remotely normalizes olfaction and hippocampal synaptic transmission. miR-200 members have multiple targets, but while an action through other pathways cannot be ruled out, similar effects can be obtained by directly replacing physiologically relevant GnRH levels. The improvement in cognitive function induced by pulsatile GnRH infusion is independent of changes in the sex steroid milieu in both DS patients and Ts65Dn mice. Similarly, in patients with congenital GnRH deficiency, who show a marked impairment of spatial ability while verbal abilities remain unchanged, these deficits are not rescued by exogenous androgen therapy (56). Conversely, inhibiting GnRHR-expressing cells in extra-hypothalamic target regions, to which hypothalamic GnRH neurons also project, leads to DS-like changes, indicating that GnRH neurons have two or more sites of action, for reproductive and non-reproductive functions, respectively.

While gonadotropin-induced gonadal function is not necessary for the cognitive or olfactory functions of GnRH, its pulsatility, necessary to regulate gonadotropin release, does appear necessary for these other functions also, and may even regulate age-related cognitive decline (57). Thus LH serum concentration and pulsatility, while not measurable in our study, may

still be a useful marker for DS-like changes (58). Similarly, in a mouse model of AD, FSH, which is elevated in DS patients and reduced by pulsatile GnRH treatment, acts directly on hippocampal neurons to mediate the AD phenotype, supporting a similar mechanism in DS (59). In that study, the effects of reducing FSH were mediated by inhibiting C/EBPβ, the product of the *Cebpb* gene, a part of the minipubertal GnRH switch that both directly and indirectly, through *Zeb1*, controls GnRH expression (18) (Fig. 3A), and whose expression was also increased in our adult trisomic mice.

Other than those genes involved in *Gnrh* expression, several genes involved in oligodendrocyte differentiation or myelination, including some that show age-related dysregulation in human DS brains, were also differentially expressed in Ts65Dn mice (12). This may explain the myelin loss observed, even though decreased brain volume and hypocellularity in DS are often attributed to a neurogenesis deficit (60). During human brain development, myelin content increases during adolescence in the cortical grey matter and to some extent in white matter (61), concomitant with improved cognition (62). Given that miR-200 in the POA normalizes the expression of myelination-related genes in the Ts65Dn mouse hippocampus, it is tempting to suggest that pulsatile GnRH secretion at puberty, a crucial hypothalamic event, could also be a signal for overall brain maturation. Some animal models of dementia, including AD, also show an upregulation of myelination genes (63) that overlap with those found in Ts65Dn mice (Fig. S19A), while genes involved in GnRH signaling are among the most downregulated in discrete cortical areas of post-mortem AD patient brains (64), as well as being dysregulated in the hippocampus of the *THY*::*TAU22* mouse AD model (65), which progressively develop a hippocampal Tau pathology in parallel with cognitive deficits (66, 67). Like adult Ts65Dn mice (Fig. 2A-C), 12-month-old male *THY*::*TAU22* mice showed normal LH pulse frequency (Fig. S19B) but decreased LH pulse amplitudes (Fig. S12C). Pulsatile Lutrelef infusion rescued odor discrimination (Fig. S12D,E) and object recognition memory (Fig. S12F) in these mice, confirming that olfactory and cognitive deficits in other neurodegenerative disorders could also be caused by the loss of GnRH and reversed by its replacement, perhaps through the same molecular pathways. Strengthening the parallels between DS and AD, *Afg3l2*, a mitochondrial gene downregulated in the Ts65Dn hippocampus, prevents both demyelination and Tau hyperphosphorylation, linking it to the AD-like phenotype observed in DS (68, 69). Additionally, mutations in *DUSP6* have been identified in patients with hypogonadotropic hypogonadism (70), but it is also hypermethylated in AD and prevents Tau hyperphosphorylation (71, 72). The differentially modulated genes identified in Ts65Dn mice thus lie at the interface between reproductive dysfunction, AD-like cognitive and neurodegenerative alterations much like the phenotype of DS patients themselves, making these mice a valuable DS model.

In terms of neuronal activity, cognitive deficits in Ts65Dn mice could result from alterations of synaptic plasticity and neurotransmission (73). Aberrant GABAergic signaling has been previously observed in Ts65Dn mice (74), as has altered long-term potentiation associated with increased hippocampal GABA release (75) and GABAergic inhibition (76, 77). Synaptic transmission in the hippocampus of our Ts65Dn mice was partly normalized by miR-200b overexpression in the septal POA, with which it is reciprocally connected (78) and which is a source of hippocampal GABAergic neurons during embryogenesis (79).

GABA is known to activate CA1 pyramidal cells in adult Ts65Dn mice, accompanied by a positive shift in the reversal potential of GABAA receptor-driven Cl^- currents and increased hippocampal expression of the cation-Cl^-cotransporter NKCC1 in both Ts65Dn mice and DS individuals (80). This suggests that the excitation-inhibition balance of hippocampal or other neuronal circuits may be perturbed in DS, resulting in impaired cognition, and that restoring physiological GnRH signaling somehow reestablishes this balance, even after the end of the developmental period. One possible molecular player underlying this mechanism is the homeoprotein Otx2, which acts as a microRNA-regulated *Gnrh1* promoter activator in the POA (18), and where it has long been suspected to play a role in maintaining GnRH expression in the adult hypothalamus as well (81). Otx2 has also been described to modulate the opening and closure of critical developmental windows for cortical GABAergic neurons at the end of the infantile period (39), raising the possibility that POA-derived Otx2 during the minipubertal GnRH switch could influence neocortical development and function. To summarize, our results provide the rationale to launch a randomized multicentric study to confirm the efficacy of pulsatile GnRH therapy in correcting the neurodevelopmental trajectory and age-related cognitive decline seen in DS and other conditions, such as AD, that share similar molecular or functional underpinnings.

Methods Summary

Animals

Male and female Ts65Dn mice (P9-P360) and their wild-type (WT) littermates were housed under specific pathogen-free conditions in a temperature-controlled room (20-21°C) with 12h light/dark cycle and ad libitum standard chow and water. Several additional transgenic mouse lines were used in this study. Animals studies were approved by the Institutional Ethics Committees for the Care and Use of Experimental animals of the Universities of Lille and Lyon 1, and the French Ministry of National Education, Higher Education and Research (APAFIS# 29172-2020121811279767 v5 and APAFIS#10164-2017060710541958 v4).

Ts65Dn mouse phenotyping—Sexual maturation and postnatal acquisition of reproductive, olfactory and cognitive impairments were assessed throughout life using external signs of puberty, hormonal profiling, olfactory discrimination, novel object recognition and visuospatial memory tests etc.

Imaging—The distribution of GnRH-immunoreactive neuronal cell bodies and projections in the brain, as well as the neocortical distribution of cells expressing the GnRH receptor promoter were assessed using both classical neuroanatomical approaches (immunofluorescence and multiplex fluorescent *in situ* hybridization) and advanced three-dimensional imaging and analysis of solvent-cleared tissue (iDISCO) methods.

Functional studies—Pharmacological (intraperitoneal administration of GnRH or CNO), viral (stereotaxic infection of the preoptic region or the hippocampus with adeno-associated viral vectors expressing Cre-dependent activatory or inhibitory DREADDs, or untargeted miR-200b) and cellular approaches (grafting dissociated newborn preoptic region cells into the hypothalamus of adult mice) were used to characterize the role of GnRH neurons and

Europe PMC Funders Author Manuscripts

secretion in the postnatal acquisition of olfactory and cognitive deficits in Ts65Dn mice. RNAseq, quantitative RT-PCR, fluorescent in situ hybridization, western blotting and *in vivo* CA1 field recordings in anesthetized mice were used to further investigate the molecular and cellular mechanisms underlying these processes.

Pulsatile GnRH treatment—Ts65Dn mice were subjected to LH pulsatile release evaluation, olfactory habituation/dishabituation and object recognition tests 1 month before and following 2 weeks of pulsatile GnRH therapy (Lutrelef®, Ferring SA, Switzerland) via a programmable subcutaneous micro-infusion pump, at a rate of 0.25 μg at 3-hr intervals to mimic the LH pulse frequency seen in male WT mice (SMP-300, iPRECIO, Japan).

Patients

Seven French-speaking men with Down syndrome (20-50 years of age) were enrolled in an open-label pilot study at Lausanne University Hospital (CHUV, Switzerland) to assess the effect of 6-month pulsatile GnRH therapy on cognitive and olfactory function (clinicaltrials.gov, NCT04390646). Written informed consent was obtained from all participants and their legal representatives prior to inclusion (Ethics Committee of Vaud, 2020-00270). Patients were subjected to baseline clinical evaluation (detailed history, physical examination, hormonal and cognitive profiling, MRI analyses) before and after 6-month pulsatile GnRH therapy via a subcutaneous pump at a rate of 75 ng/kg/pulse at 2-hr intervals (LutrePulse® manager and LutrePod®, Ferrring SA, Switzerland) to mimic LH pulse frequency in normal men. Six age-matched healthy male controls were also recruited to compare baseline parameters.

Imaging studies comprised structural MRI and resting-state functional MRI using a 3T wholebody MRI system using a 64-channel radiofrequency head and body coil for transmission (Magneton Prisma, Siemens Medical Systems, Germany).

Statistics—Data were assessed for normality and statistical differences evaluated using appropriate parametric or non-parametric tests for two or more groups.

Supplementary Material

Refer to Web version on PubMed Central for supplementary material.

Acknowledgments

The authors would like to thank PLBS UAR 2014 – US41 (https://ums-plbs.univ-lille.fr/) with its different platforms and staff for expert technical assistance: Charlotte Laloux (behavioral exploration platform for rodents), Nathalie Jouy (cell sorting Facility, BICeL), Meryem Tardivel and Antonino Bongiovanni (microscopy core facility, BICeL) and Julien Devassine (Animal house) of the UMS2014-US41 for expert technical assistance. For the technical expertise during the clinical study, the authors would also like to thank Prof. Basile Landis (Olfactology Unit, HUG), Anne-Sophie Boulin and Peggy Cazin D'Honincthun (neuropsychological tests, Neurorehabilitation Unit, CHUV), Giulia Di Domenicantonio (Dept. of Neuroclinical sciences, LREN - CHUV), Argnesa Stojkai (Dept. of Endocrinology, CHUV), and Pascal Benkert (Dept. Neuroimmunology and Neuroscience, Basel). GnRH therapy was kindly provided by Ferring SA, Switzerland.

Funding

This work has been supported by the European Research Council COST action BM1105 for the study of GnRH deficiency (to U.B., P.C., P.G., N.P., V.P., M.T.-S.), Agence Nationale de la Recherche grants ANR-17-CE16-0015 (to V.P., P.C. and L.B.), DistAlz (ANR-11-LABEX-0009 to V.P. and L.B.), I-SITE ULNE (ANR-16-IDEX-0004), the Région Rhône-Alpes- SCUSI 2018-#R18119CC and Swiss National Fund 310030B_201275 (to N.P.). M.M.-L received a postdoctoral fellowship from the European commission (H2020-MSCA-IF-2014, No 656730) and V.L. a doctoral fellowship from Inserm and the Region Hauts de France. PG is supported by the European Union's Horizon 2020 Research and Innovation Programme under grant Agreement No 874741. BD is supported by the Swiss National Science Foundation (project grant numbers 32003B_135679, 32003B_159780, 324730_192755 and CRSK-3_190185), ERA-NET iSEE project, UNIL-EPFL CLIMACT programme and the SPHN-SACR project. AL is supported by the Swiss National Science Foundation (project grant number 320030_184784) and the ROGER DE SPOELBERCH foundation. LREN is very grateful to the ROGER DE SPOELBERCH and Partridge Foundations for their generous financial support.

Data and code availability

The accession number for the RNA-seq data reported in this paper is GEO: GSE199974. All the other data supporting the findings of this study are available within the article and its supplementary information files.

References

1. Antonarakis SE, et al. Down syndrome. Nat Rev Dis Primers. 2020; 6: 9. [PubMed: 32029743]
2. de la Torre R, et al. Safety and efficacy of cognitive training plus epigallocatechin-3-gallate in young adults with Down's syndrome (TESDAD): a double-blind, randomised, placebo-controlled, phase 2 trial. Lancet Neurol. 2016; 15: 801–810. [PubMed: 27302362]
3. Shapiro BL. Down syndrome--a disruption of homeostasis. Am J Med Genet. 1983; 14: 241–269. [PubMed: 6220605]
4. Baburamani AA, Patkee PA, Arichi T, Rutherford MA. New approaches to studying early brain development in Down syndrome. Dev Med Child Neurol. 2019; 61: 867–879. [PubMed: 31102269]
5. Bull MJ. Down Syndrome. N Engl J Med. 2020; 382: 2344–2352. [PubMed: 32521135]
6. Fortea J, et al. Clinical and biomarker changes of Alzheimer's disease in adults with Down syndrome: a cross-sectional study. Lancet. 2020; 395: 1988–1997. [PubMed: 32593336]
7. Bayen E, Possin KL, Chen Y, Cleret de Langavant L, Yaffe K. Prevalence of Aging, Dementia, and Multimorbidity in Older Adults With Down Syndrome. JAMA Neurol. 2018; 75: 1399–1406. [PubMed: 30032260]
8. Antonarakis SE. Down syndrome and the complexity of genome dosage imbalance. Nat Rev Genet. 2017; 18: 147–163. [PubMed: 28029161]
9. Dierssen M. Down syndrome: the brain in trisomic mode. Nat Rev Neurosci. 2012; 13: 844–858. [PubMed: 23165261]
10. Editorial TL. Strengthening connections between Down syndrome and AD. Lancet Neurol. 2013; 12: 931. [PubMed: 24050729]
11. Lott IT, Head E. Dementia in Down syndrome: unique insights for Alzheimer disease research. Nat Rev Neurol. 2019; 15: 135–147. [PubMed: 30733618]
12. Olmos-Serrano JL, et al. Down Syndrome Developmental Brain Transcriptome Reveals Defective Oligodendrocyte Differentiation and Myelination. Neuron. 2016; 89: 1208–1222. [PubMed: 26924435]
13. Doty RL. Olfactory dysfunction in Parkinson disease. Nat Rev Neurol. 2012; 8: 329–339. [PubMed: 22584158]
14. Nijjar RK, Murphy C. Olfactory impairment increases as a function of age in persons with Down syndrome. Neurobiol Aging. 2002; 23: 65–73. [PubMed: 11755021]
15. Hsiang YH, Berkovitz GD, Bland GL, Migeon CJ, Warren AC. Gonadal function in patients with Down syndrome. Am J Med Genet. 1987; 27: 449–458. [PubMed: 2955699]

Europe PMC Funders Author Manuscripts

16. Boehm U, et al. Expert consensus document: European Consensus Statement on congenital hypogonadotropic hypogonadism--pathogenesis, diagnosis and treatment. Nat Rev Endocrinol. 2015; 11: 547–564. [PubMed: 26194704]
17. Knobil E. The GnRH pulse generator. Am J Obstet Gynecol. 1990; 163: 1721–1727. [PubMed: 2122728]
18. Messina A, et al. A microRNA switch regulates the rise in hypothalamic GnRH production before puberty. Nat Neurosci. 2016; 19: 835–844. [PubMed: 27135215]
19. Pellegrino G, et al. GnRH neurons recruit astrocytes in infancy to facilitate network integration and sexual maturation. Nat Neurosci. 2021; 24: 1660–1672. [PubMed: 34795451]
20. Lanciotti L, Cofini M, Leonardi A, Penta L, Esposito S. Up-To-Date Review About Minipuberty and Overview on Hypothalamic-Pituitary-Gonadal Axis Activation in Fetal and Neonatal Life. Front Endocrinol (Lausanne). 2018; 9: 410. [PubMed: 30093882]
21. Casoni F, et al. Development of the neurons controlling fertility in humans: new insights from 3D imaging and transparent fetal brains. Development. 2016; 143: 3969–3981. [PubMed: 27803058]
22. Skrapits K, et al. The cryptic gonadotropin-releasing hormone neuronal system of human basal ganglia. Elife. 2021; 10
23. Schang AL, et al. GnRH receptor gene expression in the developing rat hippocampus: transcriptional regulation and potential roles in neuronal plasticity. Endocrinology. 2011; 152: 568–580. [PubMed: 21123436]
24. Reeves RH, et al. A mouse model for Down syndrome exhibits learning and behaviour deficits. Nat Genet. 1995; 11: 177–184. [PubMed: 7550346]
25. Kola I, Hertzog PJ. Down syndrome and mouse models. Curr Opin Genet Dev. 1998; 8: 316–321. [PubMed: 9690992]
26. Epstein CJ, et al. Protocols to establish genotype-phenotype correlations in Down syndrome. Am J Hum Genet. 1991; 49: 207–235. [PubMed: 1829580]
27. Bianchi P, et al. Age-related impairment of olfactory bulb neurogenesis in the Ts65Dn mouse model of Down syndrome. Exp Neurol. 2014; 251: 1–11. [PubMed: 24192151]
28. Breton-Provencher V, Lemasson M, Peralta MR 3rd, Saghatelyan A. Interneurons produced in adulthood are required for the normal functioning of the olfactory bulb network and for the execution of selected olfactory behaviors. J Neurosci. 2009; 29: 15245–15257. [PubMed: 19955377]
29. Nelson L, et al. Learning and memory as a function of age in Down syndrome: a study using animal-based tasks. Prog Neuropsychopharmacol Biol Psychiatry. 2005; 29: 443–453. [PubMed: 15795053]
30. Cohen SJ, et al. The rodent hippocampus is essential for nonspatial object memory. Curr Biol. 2013; 23: 1685–1690. [PubMed: 23954431]
31. Zhang G, et al. Hypothalamic programming of systemic ageing involving IKK-beta, NF-kappaB and GnRH. Nature. 2013; 497: 211–216. [PubMed: 23636330]
32. Moore CS, et al. Increased male reproductive success in Ts65Dn “Down syndrome” mice. Mamm Genome. 2010; 21: 543–549. [PubMed: 21110029]
33. Grinspon RP, et al. Early onset of primary hypogonadism revealed by serum anti-Mullerian hormone determination during infancy and childhood in trisomy 21. Int J Androl. 2011; 34: e487–498. [PubMed: 21831236]
34. Belle M, et al. Tridimensional Visualization and Analysis of Early Human Development. Cell. 2017; 169: 161–173. e112 [PubMed: 28340341]
35. Pinto B, et al. Rescuing Over-activated Microglia Restores Cognitive Performance in Juvenile Animals of the Dp(16) Mouse Model of Down Syndrome. Neuron. 2020; 108: 887–904. e812 [PubMed: 33027640]
36. Li Z, Zhang Y, Li D, Feng Y. Destabilization and mislocalization of myelin basic protein mRNAs in quaking dysmyelination lacking the QKI RNA-binding proteins. J Neurosci. 2000; 20: 4944–4953. [PubMed: 10864952]
37. Schafer S, et al. Translational regulation shapes the molecular landscape of complex disease phenotypes. Nat Commun. 2015; 6 7200 [PubMed: 26007203]

38. Chothani S, et al. Widespread Translational Control of Fibrosis in the Human Heart by RNA-Binding Proteins. Circulation. 2019; 140: 937–951. [PubMed: 31284728]
39. Spatazza J, et al. Homeoprotein signaling in development, health, and disease: a shaking of dogmas offers challenges and promises from bench to bed. Pharmacol Rev. 2013; 65: 90–104. [PubMed: 23300132]
40. Krieger DT, et al. Brain grafts reverse hypogonadism of gonadotropin releasing hormone deficiency. Nature. 1982; 298: 468–471. [PubMed: 7045700]
41. Hoffman AR, Crowley WF Jr. Induction of puberty in men by long-term pulsatile administration of low-dose gonadotropin-releasing hormone. N Engl J Med. 1982; 307: 1237–1241. [PubMed: 6813732]
42. Hurley DM, et al. Induction of ovulation and fertility in amenorrheic women by pulsatile low-dose gonadotropin-releasing hormone. N Engl J Med. 1984; 310: 1069–1074. [PubMed: 6424012]
43. Belchetz PE, Plant TM, Nakai Y, Keogh EJ, Knobil E. Hypophysial responses to continuous and intermittent delivery of hypopthalamic gonadotropin-releasing hormone. Science. 1978; 202: 631–633. [PubMed: 100883]
44. Benkert P, et al. Serum neurofilament light chain for individual prognostication of disease activity in people with multiple sclerosis: a retrospective modelling and validation study. Lancet Neurol. 2022; 21: 246–257. [PubMed: 35182510]
45. Lee NR, et al. Hypoplasia of cerebellar afferent networks in Down syndrome revealed by DTI-driven tensor based morphometry. Sci Rep. 2020; 10 5447 [PubMed: 32214129]
46. Figueroa-Jimenez MD, et al. Resting-state default mode network connectivity in young individuals with Down syndrome. Brain Behav. 2021; 11 e01905 [PubMed: 33179859]
47. Figueroa-Jimenez MD, et al. Complexity Analysis of the Default Mode Network Using Resting-State fMRI in Down Syndrome: Relationships Highlighted by a Neuropsychological Assessment. Brain Sci. 2021; 11
48. Huang CC, et al. Age-related changes in resting-state networks of a large sample size of healthy elderly. CNS Neurosci Ther. 2015; 21: 817–825. [PubMed: 25864728]
49. Pujol J, et al. Anomalous brain functional connectivity contributing to poor adaptive behavior in Down syndrome. Cortex. 2015; 64: 148–156. [PubMed: 25461715]
50. Goeldner C, et al. A randomized, double-blind, placebo-controlled phase II trial to explore the effects of a GABAA-alpha5 NAM (basmisanil) on intellectual disability associated with Down syndrome. J Neurodev Disord. 2022; 14: 10. [PubMed: 35123401]
51. Hanney M, et al. Memantine for dementia in adults older than 40 years with Down's syndrome (MEADOWS): a randomised, double-blind, placebo-controlled trial. Lancet. 2012; 379: 528–536. [PubMed: 22236802]
52. McShane R, Areosa Sastre A, Minakaran N. Memantine for dementia. Cochrane Database Syst Rev. 2006. CD003154 [PubMed: 16625572]
53. Boada R, et al. Antagonism of NMDA receptors as a potential treatment for Down syndrome: a pilot randomized controlled trial. Transl Psychiatry. 2012; 2: e141. [PubMed: 22806212]
54. Carr J. Stability and change in cognitive ability over the life span: a comparison of populations with and without Down's syndrome. J Intellect Disabil Res. 2005; 49: 915–928. [PubMed: 16287480]
55. Ballard C, Mobley W, Hardy J, Williams G, Corbett A. Dementia in Down's syndrome. Lancet Neurol. 2016; 15: 622–636. [PubMed: 27302127]
56. Hier DB, Crowley WF Jr. Spatial ability in androgen-deficient men. N Engl J Med. 1982; 306: 1202–1205. [PubMed: 7070432]
57. Wang Z, Wu W, Kim SK, Cai D. GnRH pulse frequency and irregularity play a role in male aging. Nature aging. 2021; 1: 904–918.
58. Moenter SM, Evans NP. Gonadotropin-releasing hormone (GnRH) measurements in pituitary portal blood: A history. J Neuroendocrinol. 2021. e13065 [PubMed: 34918405]
59. Xiong J, et al. FSH blockade improves cognition in mice with Alzheimer's disease. Nature. 2022; 603: 470–476. [PubMed: 35236988]

60. Guidi S, Ciani E, Bonasoni P, Santini D, Bartesaghi R. Widespread proliferation impairment and hypocellularity in the cerebellum of fetuses with down syndrome. Brain Pathol. 2011; 21: 361–373. [PubMed: 21040072]
61. Corrigan NM, et al. Myelin development in cerebral gray and white matter during adolescence and late childhood. Neuroimage. 2021; 227 117678 [PubMed: 33359342]
62. Kwon D, Pfefferbaum A, Sullivan EV, Pohl KM. Regional growth trajectories of cortical myelination in adolescents and young adults: longitudinal validation and functional correlates. Brain Imaging Behav. 2020; 14: 242–266. [PubMed: 30406353]
63. Benito E, et al. HDAC inhibitor-dependent transcriptome and memory reinstatement in cognitive decline models. J Clin Invest. 2015; 125: 3572–3584. [PubMed: 26280576]
64. Wang M, et al. Integrative network analysis of nineteen brain regions identifies molecular signatures and networks underlying selective regional vulnerability to Alzheimer's disease. Genome Med. 2016; 8: 104. [PubMed: 27799057]
65. Chatterjee S, et al. Reinstating plasticity and memory in a tauopathy mouse model with an acetyltransferase activator. EMBO Mol Med. 2018; 10
66. Schindowski K, et al. Alzheimer's disease-like tau neuropathology leads to memory deficits and loss of functional synapses in a novel mutated tau transgenic mouse without any motor deficits. Am J Pathol. 2006; 169: 599–616. [PubMed: 16877359]
67. Van der Jeugd A, et al. Progressive age-related cognitive decline in tau mice. J Alzheimers Dis. 2013; 37: 777–788. [PubMed: 23948912]
68. Kondadi AK, et al. Loss of the m-AAA protease subunit AFG(3)L(2) causes mitochondrial transport defects and tau hyperphosphorylation. EMBO J. 2014; 33: 1011–1026. [PubMed: 24681487]
69. Wang S, et al. The Mitochondrial m-AAA Protease Prevents Demyelination and Hair Greying. PLoS Genet. 2016; 12 e1006463 [PubMed: 27911893]
70. Miraoui H, et al. Mutations in FGF17, IL17RD, DUSP6, SPRY4, and FLRT3 are identified in individuals with congenital hypogonadotropic hypogonadism. Am J Hum Genet. 2013; 92: 725–743. [PubMed: 23643382]
71. Liu Y, Wang M, Marcora EM, Zhang B, Goate AM. Promoter DNA hypermethylation - Implications for Alzheimer's disease. Neurosci Lett. 2019; 711 134403 [PubMed: 31351091]
72. Banzhaf-Strathmann J, et al. MicroRNA-125b induces tau hyperphosphorylation and cognitive deficits in Alzheimer's disease. EMBO J. 2014; 33: 1667–1680. [PubMed: 25001178]
73. Cramer N, Galdzicki Z. From abnormal hippocampal synaptic plasticity in down syndrome mouse models to cognitive disability in down syndrome. Neural Plast. 2012; 2012 101542 [PubMed: 22848844]
74. Deidda G, et al. Reversing excitatory GABAAR signaling restores synaptic plasticity and memory in a mouse model of Down syndrome. Nat Med. 2015; 21: 318–326. [PubMed: 25774849]
75. Begenisic T, et al. Fluoxetine in adulthood normalizes GABA release and rescues hippocampal synaptic plasticity and spatial memory in a mouse model of Down syndrome. Neurobiol Dis. 2014; 63: 12–19. [PubMed: 24269730]
76. Schulz JM, Knoflach F, Hernandez MC, Bischofberger J. Enhanced Dendritic Inhibition and Impaired NMDAR Activation in a Mouse Model of Down Syndrome. J Neurosci. 2019; 39: 5210–5221. [PubMed: 31000585]
77. Freeburn A, Munn RGK. Signalling pathways contributing to learning and memory deficits in the Ts65Dn mouse model of Down syndrome. Neuronal Signal. 2021; 5 NS20200011 [PubMed: 33763235]
78. Swanson LW, Cowan WM. The connections of the septal region in the rat. J Comp Neurol. 1979; 186: 621–655. [PubMed: 15116692]
79. Gelman DM, et al. The embryonic preoptic area is a novel source of cortical GABAergic interneurons. J Neurosci. 2009; 29: 9380–9389. [PubMed: 19625528]
80. Deidda G, et al. Early depolarizing GABA controls critical-period plasticity in the rat visual cortex. Nat Neurosci. 2015; 18: 87–96. [PubMed: 25485756]

81. Kelley CG, Lavorgna G, Clark ME, Boncinelli E, Mellon PL. The Otx2 homeoprotein regulates expression from the gonadotropin-releasing hormone proximal promoter. Mol Endocrinol. 2000; 14: 1246–1256. [PubMed: 10935548]
82. Prevot, V, Messina, A, Giacobini, P, Leysen, V, Manfredi-Lozano, M. WO/2020/221821. Inserm. , editor. France: 2020. chap. PCT/EP2020/061943
83. Ahmed MM, Sturgeon X, Ellison M, Davisson MT, Gardiner KJ. Loss of correlations among proteins in brains of the Ts65Dn mouse model of down syndrome. J Proteome Res. 2012; 11: 1251–1263. [PubMed: 22214338]
84. Reinholdt LG, et al. Molecular characterization of the translocation breakpoints in the Down syndrome mouse model Ts65Dn. Mamm Genome. 2011; 22: 685–691. [PubMed: 21953412]
85. Yoon H, Enquist LW, Dulac C. Olfactory inputs to hypothalamic neurons controlling reproduction and fertility. Cell. 2005; 123: 669–682. [PubMed: 16290037]
86. Harfe BD, McManus MT, Mansfield JH, Hornstein E, Tabin CJ. The RNaseIII enzyme Dicer is required for morphogenesis but not patterning of the vertebrate limb. Proc Natl Acad Sci U S A. 2005; 102: 10898–10903. [PubMed: 16040801]
87. Spergel DJ, Kruth U, Hanley DF, Sprengel R, Seeburg PH. GABA- and glutamate-activated channels in green fluorescent protein-tagged gonadotropin-releasing hormone neurons in transgenic mice. J Neurosci. 1999; 19: 2037–2050. [PubMed: 10066257]
88. Hoffmann HM, et al. Differential CRE Expression in Lhrh-cre and GnRH-cre Alleles and the Impact on Fertility in Otx2-Flox Mice. Neuroendocrinology. 2019; 108: 328–342. [PubMed: 30739114]
89. Slezak M, et al. Relevance of exocytotic glutamate release from retinal glia. Neuron. 2012; 74: 504–516. [PubMed: 22578502]
90. Wen S, Ai W, Alim Z, Boehm U. Embryonic gonadotropin-releasing hormone signaling is necessary for maturation of the male reproductive axis. Proc Natl Acad Sci U S A. 2010; 107: 16372–16377. [PubMed: 20805495]
91. Steyn FJ, et al. Development of a methodology for and assessment of pulsatile luteinizing hormone secretion in juvenile and adult male mice. Endocrinology. 2013; 154: 4939–4945. [PubMed: 24092638]
92. Vidal A, Zhang Q, Medigue C, Fabre S, Clement F. DynPeak: an algorithm for pulse detection and frequency analysis in hormonal time series. PLoS One. 2012; 7 e39001 [PubMed: 22802933]
93. Scattoni ML, Gandhy SU, Ricceri L, Crawley JN. Unusual repertoire of vocalizations in the BTBR T+tf/J mouse model of autism. PLoS One. 2008; 3 e3067 [PubMed: 18728777]
94. Leger M, et al. Object recognition test in mice. Nat Protoc. 2013; 8: 2531–2537. [PubMed: 24263092]
95. Bridoux A, Laloux C, Derambure P, Bordet R, Monaca Charley C. The acute inhibition of rapid eye movement sleep by citalopram may impair spatial learning and passive avoidance in mice. J Neural Transm (Vienna). 2013; 120: 383–389. [PubMed: 23053350]
96. Dellu F, Contarino A, Simon H, Koob GF, Gold LH. Genetic differences in response to novelty and spatial memory using a two-trial recognition task in mice. Neurobiol Learn Mem. 2000; 73: 31–48. [PubMed: 10686122]
97. Livak KJ, Schmittgen TD. Analysis of relative gene expression data using real-time quantitative PCR and the 2(-Delta Delta C(T)) Method. Methods. 2001; 25: 402–408. [PubMed: 11846609]
98. Paxinos, G, Franklin, KBJ. The mouse brain in stereotaxic coordinates. Academic Press; London: 2004.
99. Dobin A, et al. STAR: ultrafast universal RNA-seq aligner. Bioinformatics. 2013; 29: 15–21. [PubMed: 23104886]
100. Anders S, Pyl PT, Huber W. HTSeq--a Python framework to work with high-throughput sequencing data. Bioinformatics. 2015; 31: 166–169. [PubMed: 25260700]
101. Wang L, Wang S, Li W. RSeQC: quality control of RNA-seq experiments. Bioinformatics. 2012; 28: 2184–2185. [PubMed: 22743226]
102. Love MI, Huber W, Anders S. Moderated estimation of fold change and dispersion for RNA-seq data with DESeq2. Genome Biol. 2014; 15: 550. [PubMed: 25516281]

Europe PMC Funders Author Manuscripts

103. Leek JT. svaseq: removing batch effects and other unwanted noise from sequencing data. Nucleic Acids Res. 2014; 42

104. Ignatiadis N, Klaus B, Zaugg JB, Huber W. Data-driven hypothesis weighting increases detection power in genome-scale multiple testing. Nat Methods. 2016; 13: 577–580. [PubMed: 27240256]

105. Tuscher JJ, Taxier LR, Fortress AM, Frick KM. Chemogenetic inactivation of the dorsal hippocampus and medial prefrontal cortex, individually and concurrently, impairs object recognition and spatial memory consolidation in female mice. Neurobiol Learn Mem. 2018; 156: 103–116. [PubMed: 30408525]

106. Hanchate NK, et al. SEMA3A, a Gene Involved in Axonal Pathfinding, Is Mutated in Patients with Kallmann Syndrome. PLoS Genet. 2012; 8 e1002896 [PubMed: 22927827]

107. Messina A, et al. Dysregulation of Semaphorin7A/beta1-integrin signaling leads to defective GnRH-1 cell migration, abnormal gonadal development and altered fertility. Hum Mol Genet. 2011; 20: 4759–4774. [PubMed: 21903667]

108. Hrabovszky E, et al. Sexual dimorphism of kisspeptin and neurokinin B immunoreactive neurons in the infundibular nucleus of aged men and women. Front Endocrinol (Lausanne). 2011; 2: 80. [PubMed: 22654828]

109. Beauvillain JC, Tramu G. Immunocytochemical demonstration of LH-RH, somatostatin, and ACTH-like peptide in osmium-postfixed, resin-embedded median eminence. J Histochem Cytochem. 1980; 28: 1014–1017. [PubMed: 6157712]

110. Erturk A, et al. Three-dimensional imaging of solvent-cleared organs using 3DISCO. Nat Protoc. 2012; 7: 1983–1995. [PubMed: 23060243]

111. Erturk A, Bradke F. High-resolution imaging of entire organs by 3-dimensional imaging of solvent cleared organs (3DISCO). Exp Neurol. 2013; 242: 57–64. [PubMed: 23124097]

112. Belle M, et al. A simple method for 3D analysis of immunolabeled axonal tracts in a transparent nervous system. Cell Rep. 2014; 9: 1191–1201. [PubMed: 25456121]

113. Mosbah H, et al. GnRH stimulation testing and serum inhibin B in males: insufficient specificity for discriminating between congenital hypogonadotropic hypogonadism from constitutional delay of growth and puberty. Hum Reprod. 2020; 35: 2312–2322. [PubMed: 32862222]

114. Noll C, et al. DYRK1A, a novel determinant of the methionine-homocysteine cycle in different mouse models overexpressing this Down-syndrome-associated kinase. PLoS One. 2009; 4 e7540 [PubMed: 19844572]

115. Nasreddine ZS, et al. The Montreal Cognitive Assessment, MoCA: a brief screening tool for mild cognitive impairment. J Am Geriatr Soc. 2005; 53: 695–699. [PubMed: 15817019]

116. De Renzi E, Vignolo LA. The token test: A sensitive test to detect receptive disturbances in aphasics. Brain. 1962; 85: 665–678. [PubMed: 14026018]

117. Cecchini MP, et al. Olfaction in People with Down Syndrome: A Comprehensive Assessment across Four Decades of Age. PLoS One. 2016; 11 e0146486 [PubMed: 26730728]

118. Ware J Jr, Kosinski M, Keller SD. A 12-Item Short-Form Health Survey: construction of scales and preliminary tests of reliability and validity. Med Care. 1996; 34: 220–233. [PubMed: 8628042]

119. Pitteloud N, et al. The relative role of gonadal sex steroids and gonadotropin-releasing hormone pulse frequency in the regulation of follicle-stimulating hormone secretion in men. J Clin Endocrinol Metab. 2008; 93: 2686–2692. [PubMed: 18445673]

120. Weiskopf N, et al. Quantitative multi-parameter mapping of R1, PD(*), MT, and R2(*) at 3T: a multi-center validation. Front Neurosci. 2013; 7: 95. [PubMed: 23772204]

121. Lutti A, Hutton C, Finsterbusch J, Helms G, Weiskopf N. Optimization and validation of methods for mapping of the radiofrequency transmit field at 3T. Magn Reson Med. 2010; 64: 229–238. [PubMed: 20572153]

122. Lutti A, et al. Robust and fast whole brain mapping of the RF transmit field B1 at 7T. PLoS One. 2012; 7 e32379 [PubMed: 22427831]

123. Helms G, Dathe H, Dechent P. Quantitative FLASH MRI at 3T using a rational approximation of the Ernst equation. Magn Reson Med. 2008; 59: 667–672. [PubMed: 18306368]

124. Helms G, Dathe H, Kallenberg K, Dechent P. High-resolution maps of magnetization transfer with inherent correction for RF inhomogeneity and T1 relaxation obtained from 3D FLASH MRI. Magn Reson Med. 2008; 60: 1396–1407. [PubMed: 19025906]
125. Tabelow K, et al. hMRI - A toolbox for quantitative MRI in neuroscience and clinical research. Neuroimage. 2019; 194: 191–210. [PubMed: 30677501]
126. Zaitsev M, Dold C, Sakas G, Hennig J, Speck O. Magnetic resonance imaging of freely moving objects: prospective real-time motion correction using an external optical motion tracking system. Neuroimage. 2006; 31: 1038–1050. [PubMed: 16600642]
127. Maclaren J, et al. Measurement and correction of microscopic head motion during magnetic resonance imaging of the brain. PLoS One. 2012; 7 e48088 [PubMed: 23144848]
128. Castella R, et al. Controlling motion artefact levels in MR images by suspending data acquisition during periods of head motion. Magn Reson Med. 2018; 80: 2415–2426. [PubMed: 29687919]
129. Lutti A, et al. Restoring statistical validity in group analyses of motion-corrupted MRI data. Hum Brain Mapp. 2022; 43: 1973–1983. [PubMed: 35112434]
130. Ashburner J, Ridgway GR. Symmetric diffeomorphic modeling of longitudinal structural MRI. Front Neurosci. 2012; 6: 197. [PubMed: 23386806]
131. Gyger L, et al. Temporal trajectory of brain tissue property changes induced by electroconvulsive therapy. Neuroimage. 2021; 232 117895 [PubMed: 33617994]
132. Draganski B, et al. Regional specificity of MRI contrast parameter changes in normal ageing revealed by voxel-based quantification (VBQ). Neuroimage. 2011; 55: 1423–1434. [PubMed: 21277375]
133. Lutti A, Thomas DL, Hutton C, Weiskopf N. High-resolution functional MRI at 3 T: 3D/2D echo-planar imaging with optimized physiological noise correction. Magn Reson Med. 2013; 69: 1657–1664. [PubMed: 22821858]
134. Weitzdoerfer R, Fountoulakis M, Lubec G. Reduction of actin-related protein complex 2/3 in fetal Down syndrome brain. Biochem Biophys Res Commun. 2002; 293: 836–841. [PubMed: 12054546]
135. Wei Y. Comparative transcriptome analysis of the hippocampus from sleep-deprived and Alzheimer's disease mice. Genet Mol Biol. 2020; 43 e20190052 [PubMed: 32338274]
136. Rao LV, Cleveland RP, Kimmel RJ, Ataya KM. Hematopoietic stem cell antigen-1 (Sca-1) expression in different lymphoid tissues of female mice treated with GnRH agonist. Am J Reprod Immunol. 1995; 34: 257–266. [PubMed: 8579764]
137. Sergeant N, et al. Progressive decrease of amyloid precursor protein carboxy terminal fragments (APP-CTFs), associated with tau pathology stages, in Alzheimer's disease. J Neurochem. 2002; 81: 663–672. [PubMed: 12065626]
138. Buée-Scherrer, et al. AD2, a phosphorylation-dependent monoclonal antibody directed against tau proteins found in Alzheimer's disease. Brain Res Mol Brain Res. 1996; 39: 79–88. [PubMed: 8804716]

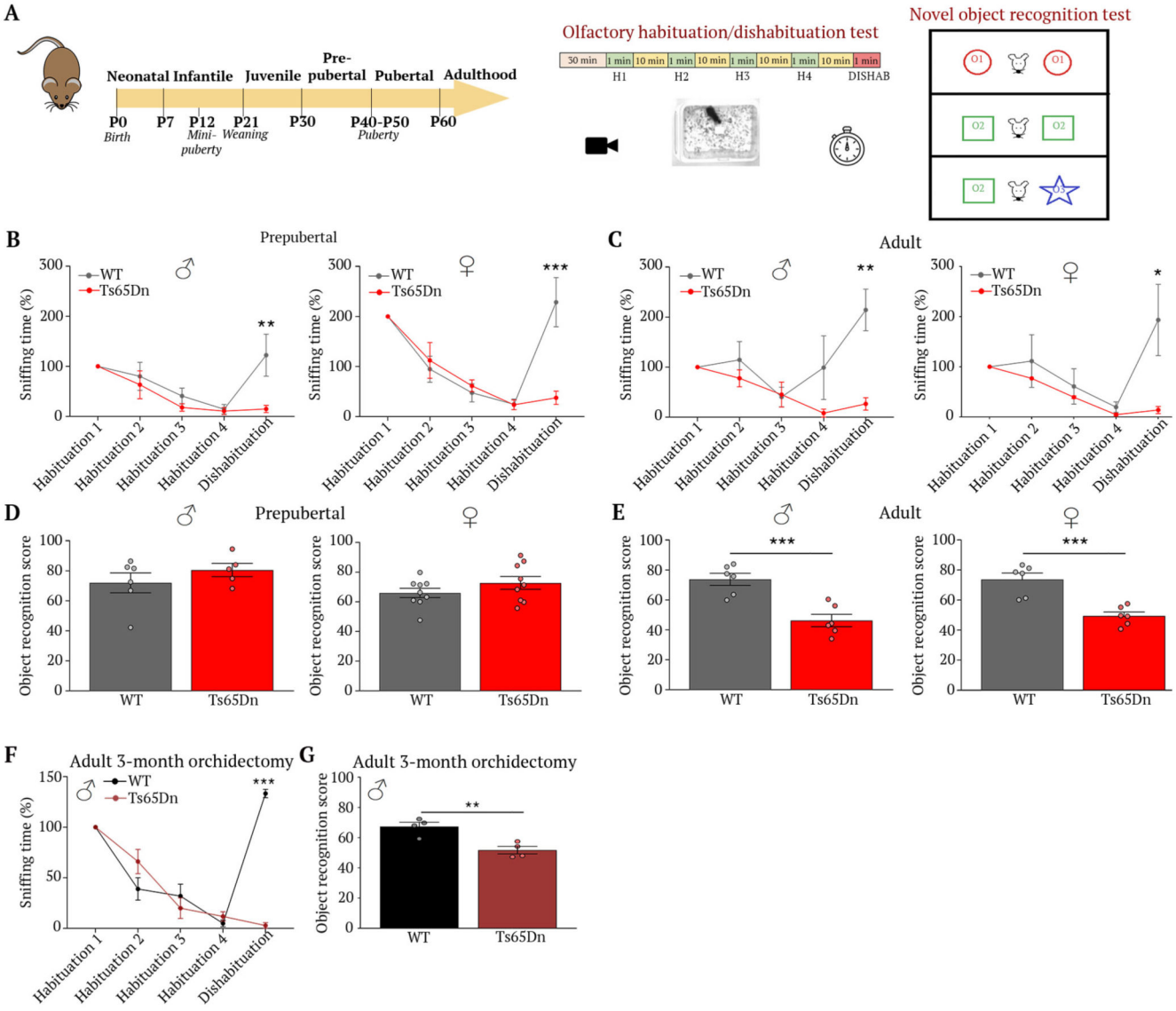

Fig. 1. Ts65Dn mice show age-dependent olfactory, cognitive loss.

(**A**) Experimental design to evaluate olfactory and visual discrimination during postnatal development. (**B-E**) Habituation/dishabituation test to assess the ability of P35 and adult Ts65Dn mice and WT littermates to differentiate between two distinct odors (P35: **B**: WT male dishabituation vs. Ts65Dn male dishabituation, $t_{(45)} = 3.67$, $P = 0.003$, n=6,5; WT female dishabituation vs. Ts65Dn female dishabituation, $t_{(105)} = 6.10$, $P < 0.0001$, n=6,5. Adult: **C**: WT male dishabituation vs. Ts65Dn male dishabituation, $t_{(45)} = 4.19$, $P = 0.0006$, n=6,5; WT female dishabituation vs. Ts65Dn female dishabituation, $t_{(16)} = 5.42$, $P = 0.0002$, n=5,5); or recognize new objects in their environment (P35: **D**: WT male vs. Ts65Dn male, $t_{(9)} = 1.02$, $P = 0.33$, n=6,5; WT female vs. Ts65Dn female, $t_{(16)} = 1.278$, $P = 0.22$, n=9,9. **E**: WT male vs. Ts65Dn male, $t_{(10)} = 4.8$, $P = 0.0007$, n=6,6; WT female vs. Ts65Dn female, $t_{(10)} = 4.93$, $P = 0.0006$, n=6,6). Values represent means ± SEM. Unpaired Student's t-test

to compare 2 conditions; two-way repeated-measures ANOVA followed by Sidak's post hoc test for ≥ 3 conditions. ** $P<0.01$; *** $P<0.001$.

Europe PMC Funders Author Manuscripts

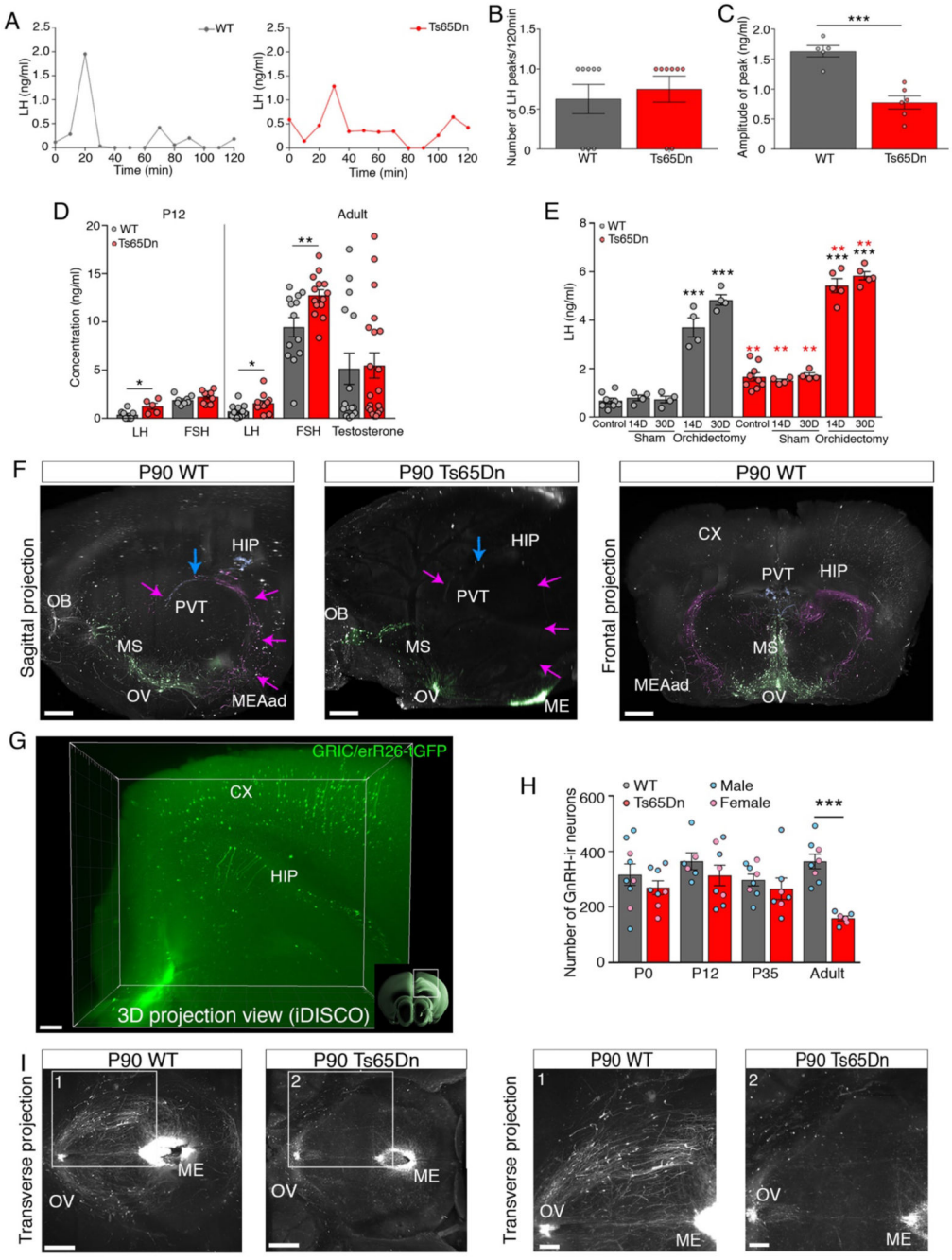

Fig. 2. Ts65Dn mice progressively lose GnRH expression, function.

(**A**) LH pulsatility assessment by serial blood sampling. (**B**) LH pulse frequency (n=8,8 mice). (**C**) LH pulse amplitude (n=5,6 mice). (**D**) Circulating levels of LH, FSH (at P12 and in adults) and testosterone (in adults) (WT n=8,12,8,13,15 mice; Ts65Dn n=5,12,9,14,20 mice). (**E**) Effect of orchidectomy on LH levels 14 days (14D) and 30 days (30D) after surgery (WT: n=8,4,4,4,4 mice; Ts65Dn: n=9,4,4,5,5 mice). (**F**) GnRH-immunoreactive neuronal fiber tracing, pseudocolored projection pathways. Green: GnRH neurons and projections to median eminence (ME); magenta: neuronal projections to the anterodorsal

Europe PMC Funders Author Manuscripts

amygdala (MEAad); blue: neuronal projections to the paraventricular thalamus (PVT). CX: cortex; HIP: hippocampus; MS: medial septum; OB: olfactory bulb; OV: organum vasculosum laminae terminalis; PVT: paraventricular thalamus. Scale bars: sagittal 350 μm; frontal 500 μm. (**G**) Three-dimensional imaging of solvent-cleared organs (iDISCO) showing Cre-dependent Tau-GFP expression in mouse neurons of the CX and HIP, under the control of the GnRH receptor (*Gnrhr*) promoter. Scale bar: 200 μm (**H**) GnRH-immunoreactive cell bodies in the preoptic region of WT and Ts65Dn mice at different postnatal ages assessed by conventional neuroanatomical analyses (WT, n=9,6,8,8 mice; Ts65Dn n=8,8,7,6 mice). (**I**) Representative horizontal view of whole-mount GnRH immunoreactivity in adult (P90) Ts65Dn and WT littermates followed by iDISCO. Scale bars: 600 μm (panels 1, 2: 300 μm).

Values represent means ± SEM. **P*<0.05; ***P*< 0.01; ****P*<0.001. Unpaired Student's *t*-test (**C**,**D**,$\mathbf{E}_{\text{red-asterisks}}$,**H**) or Mann-Whitney U test for comparison between 2 conditions (**B**,**D**); one-way ANOVA followed by Tukey's post hoc test for ≥ 3 conditions (**E**). Red asterisks indicate a comparison between genotypes.

Europe PMC Funders Author Manuscripts

Europe PMC Funders Author Manuscripts

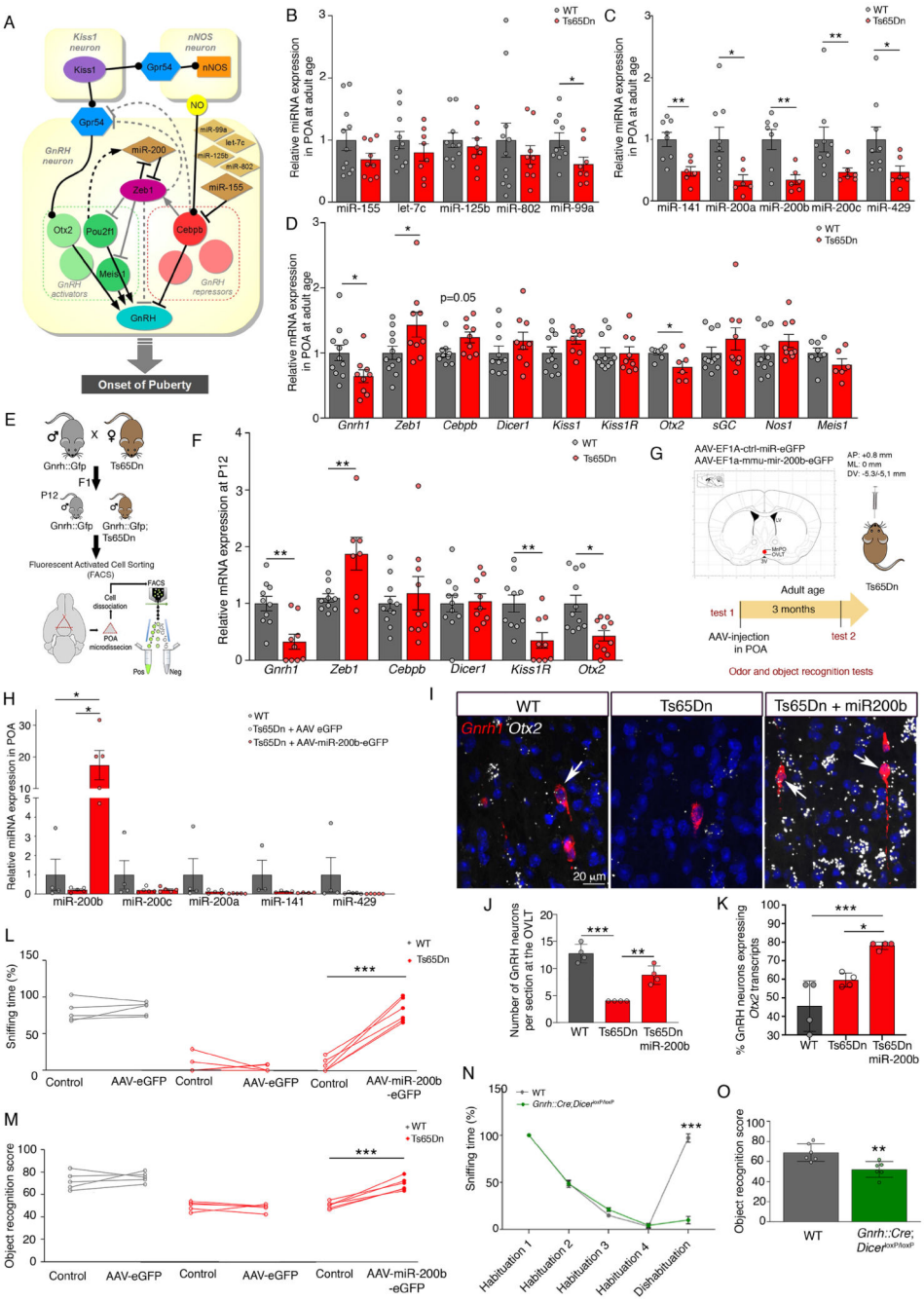

Fig. 3. GnRH transcriptional machinery disequilibrium underlies cognitive impairments.

(**A**) Putative microRNA-transcription-factor network regulating hypothalamic GnRH promoter activation during postnatal development (adapted from (18)). (**B**-**D**) RT-PCR analysis of expression levels of microRNAs located on chromosome 16 (**B**) and miR-200 family members (**C**), as well as hypothalamic GnRH promoter modulators (**D**) in the preoptic region (POA) of adult WT and Ts65Dn littermates (**B**: n=11,10,10,11,10 WT mice; n=9,8,8,9,8 Ts65Dn mice; **C**: n=8,9,7,9,9 WT mice; n=6,6,6,6,6 Ts65Dn mice; **D**: n=11,11,9,10,11,11,7,11,11,8 WT mice; n=9,9,9,9,9,9,6,9,9,6 Ts65Dn mice). (**E**)

Generation of *Gnrh::Gfp;Ts65Dn* reporter mice, which express GFP under an ectopic *Gnrh* promoter. GnRH-GFP neurons were FACS-isolated from the POA of *Gnrh::Gfp* and *Gnrh::Gfp*;Ts65Dn littermates at P12. (**F**) RT-PCR analysis of gene expression in FACS-sorted GnRH-GFP cells (n=10,10,11,11,10,11 WT mice; n=9,7,9,9,9,10 Ts65Dn mice). (**G**) Experimental design to evaluate the functional involvement of miR-200 family members in odor discrimination and novel object recognition in Ts65Dn mice. Red dot: viral injection site; LV, lateral ventricle; MePO, median preoptic nucleus; OVLT, organum vasculosum laminae terminalis. (**H**) Effect of viral overexpression of miR-200b in the POA on miR-200 family member expression (n=4,5,5 mice). (**I**-**M**) Effect of viral miR-200b overexpression in the POA on the number of neurons expressing *Gnrh* transcripts in the OVLT (**I,J**) and the proportion expressing *Otx2* (**I,K**), as assessed by fluorescent in situ hybridization, as well as odor discrimination (**L**) and novel object recognition (**M**) in Ts65Dn mice (**J**,**K**; n=4,4,4 mice; **L,M**: n=5,5,6 mice). (**N**,**O**) Odor discrimination (**N**; n=6 per group) and novel object recognition (**O**; n=6 per group) in 12-month old male mice selectively lacking Dicer in GnRH neurons.

Values represent means ± SEM. **P*<0.05; ***P*<0.01; ****P*<0.001. Unpaired Student's-test or Mann-Whitney U test (**B**-**D**,**F**), paired Student's-test or Wilcoxon matched-pair test (**L**,**M**) and Kruskal-Wallis test (**H**) for comparisons between 2 conditions, one-way (J,K) or two-way repeated measures (**N**,**O**) ANOVA followed by Tukey's and Sidak's post hoc tests for ≥ 3 conditions.

Europe PMC Funders Author Manuscripts

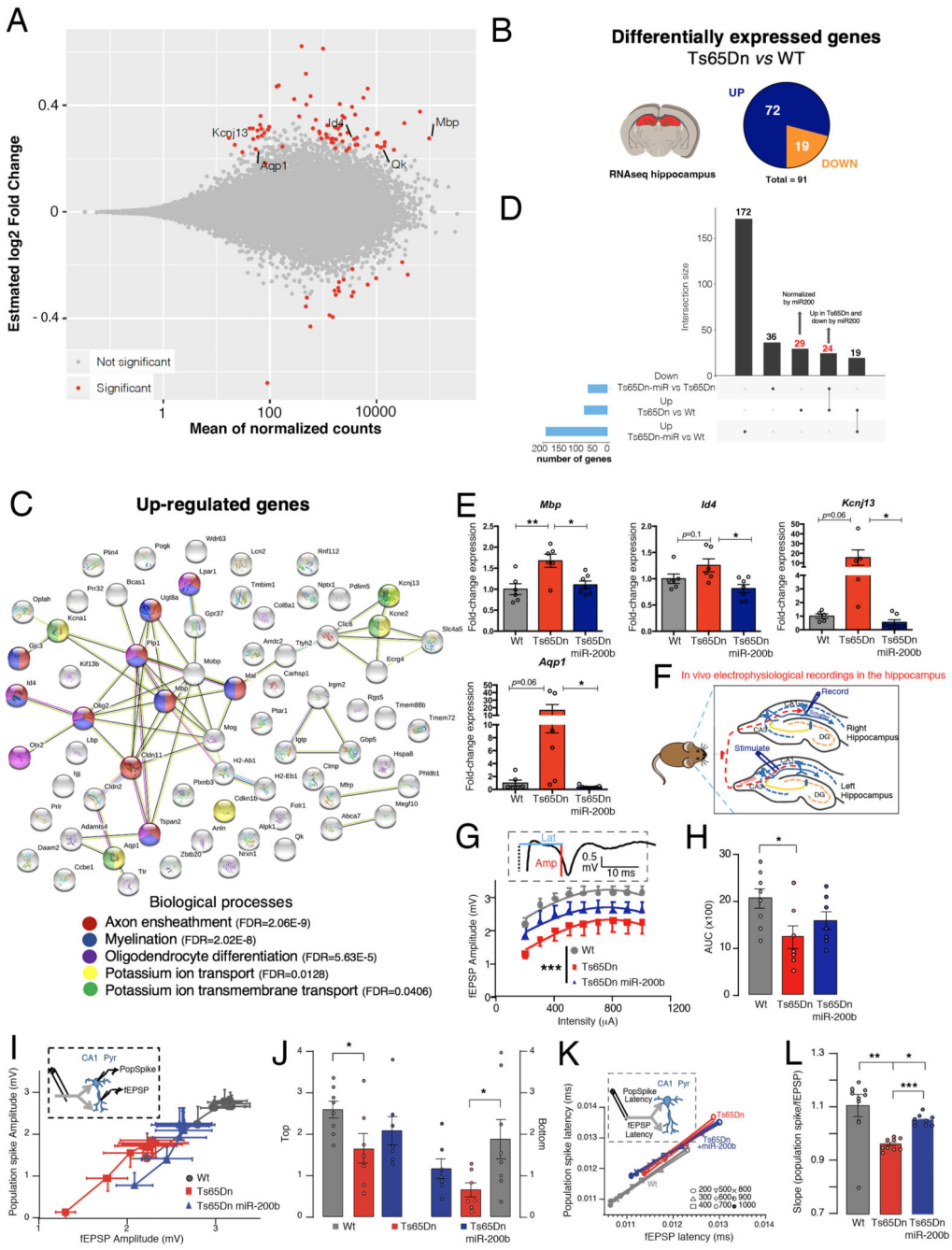

Fig. 4. Hypothalamic miR-200b overexpression rescues hippocampal transcriptome, connectivity.

(**A**)MA plot of gene expression changes (estimated $\log_2$ fold changes as a function of the mean of normalized counts; P_{Adj}<0.05) in the hippocampus of adult male (P180) Ts65Dn (n=3) vs. WT mice (n=4). (**B**) Pie chart of the number of differentially regulated genes between Ts65Dn and WT littermates in the hippocampus (P_{adj}<0.05). (**C**) STRING protein network analysis of upregulated genes. (**D**) UpSet plot showing the intersection between differentially up-regulated genes in the Ts65Dn hippocampus and genes rescued by miR-200b. (**E**) Quantitative RT-PCR confirmation of RNA-seq data. (**F**) Schematic

diagram illustrating in vivo electrophysiological recordings in the dorsal hippocampus of adult WT (n=8), Ts65Dn (n=7) and Ts65Dn mice with miR-200b overexpression (n=7). Field excitatory postsynaptic potentials (fEPSPs) and population spikes were evoked in the hippocampal CA1 area by stimulating commissural fibers in the contralateral hippocampus. (**G**) Synaptic input-output (I/O) curves indicating the relationship between fEPSP amplitude at increasing stimulus intensities (200-1000 μA). Insert: Representative fEPSP recording with measurement of latency (blue line) and amplitude (red line). **(H)** Area under the curve (AUC) of fEPSP responses. (**I**) Boltzmann-fitted fEPSP-population spike coupling. Insert: schematic showing both fEPSP and population spike recording in the CA1 pyramidal layer (CA1 pyr) following the same commissural path stimulation. (**J**) Top and bottom Boltzmann-fitted parameters of fEPSP-population spike coupling as a measure of intrinsic excitability of CA1 pyramidal neurons. (**K**) Relationship between the mean fEPSP latency and population spike latency at different stimulus intensities (200-1000 μA). Insert: schematic showing both fEPSP and population spike recording in the CA1 pyramidal layer (CA1 pyr) following the same commissural path stimulation. (**L**): Slopes of the fEPSP-population spike relationships. Data represent means ± SEM. *$P \leq 0.05$; **$P \leq 0.01$;***$P \leq 0.001$. Kruskal-Wallis ANOVA and Mann-Whitney U test (**G**) for comparisons between two conditions, one-way ANOVA followed by Tukey's post hoc test (**E**,**H**,**L**) or two-way ANOVA (**J**) for ≥ 3 conditions.

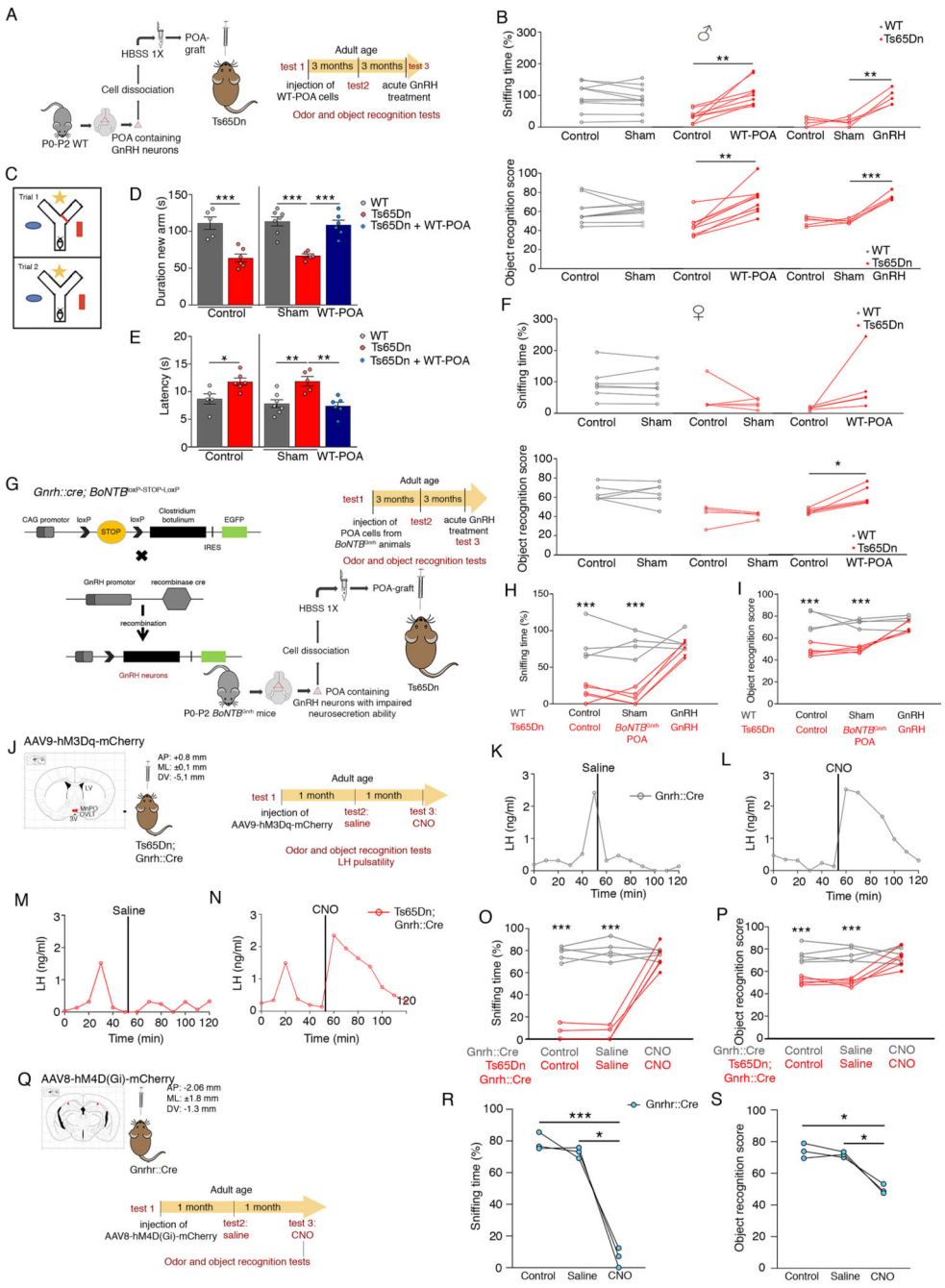

Fig. 5. Restoring GnRH neurons/function reverses olfactory, cognitive deficits.

(**A**) Cell therapy by grafting enzymatically dissociated cells from the POA of WT neonatal mice (P0-P2) into the third ventricle of adult Ts65Dn mice. (**B-F**) Effect of WT-POA grafts in Ts65Dn males on olfactory and cognitive performance (**B**: n=10,9,5 male mice; **F**: n=7,5,5 female mice) and short-term visuospatial memory assessed by the Y-maze test (**C-E**) 3 months after surgery (**D**: n=5,6,7,5,7 male mice; **E**: n=5,6,7,5,6 male mice). (**G**) Experimental design to graft POA cells from neonatal mice with exocytotis-incompetent GnRH neurons (*Gnrh::Cre*; *BoNTB*$^{loxP\text{-}STOP\text{-}loxP}$). (**H,I**) After a 3-month recovery period,

Europe PMC Funders Author Manuscripts

effect of *BoNTB*^{Gnrh}-POA grafts and acute intraperitoneal GnRH injection on odor discrimination (**H**) and object recognition (**I**) (**H**,**I**: n=4,5 mice). (**J**) Experimental design to study LH pulsatility, cognitive and olfactory performance after the chemogenetic activation of GnRH neurons by injecting adult *Gnrh::Cre* and Ts65Dn;*Gnrh::Cre* mice with an hM3Dq DREADD viral vector followed by CNO (clozapine N-oxide solution; 1mg/kg of body weight) (n=5,5 mice). Red dots: virus injection sites. 3V: third ventricle; LV: lateral ventricle; MePO: median preoptic nucleus; OVLT: organum vasculosum laminae terminalis. (**K-N**) Representative graphs for LH pulsatility; (**O**) odor discrimination; (**P**) novel object recognition. (**Q**) Experimental design to study olfactory and cognitive performance before and after the chemogenetic inhibition of GnRH-R expressing neurons in 6-month old *Gnrhr::Cre* mice by injection of an hM4D(Gi) DREADD viral vector. Red dots: virus injection sites. (**R**) Odor discrimination; (**S**) novel object recognition (n=3,3 mice). Values represent means ± SEM. * $P<0.05$,** $P<0.01$,*** $P<0.001$; paired Student's *t*-test or Wilcoxon matched-pair test (**F**); one-way ANOVA (**D,E**) or oneway (**R,S**) or two-way (**B,H,I,O,P**) repeated-measures ANOVA followed by Tukey's or Sidak's post hoc tests, respectively.

Europe PMC Funders Author Manuscripts

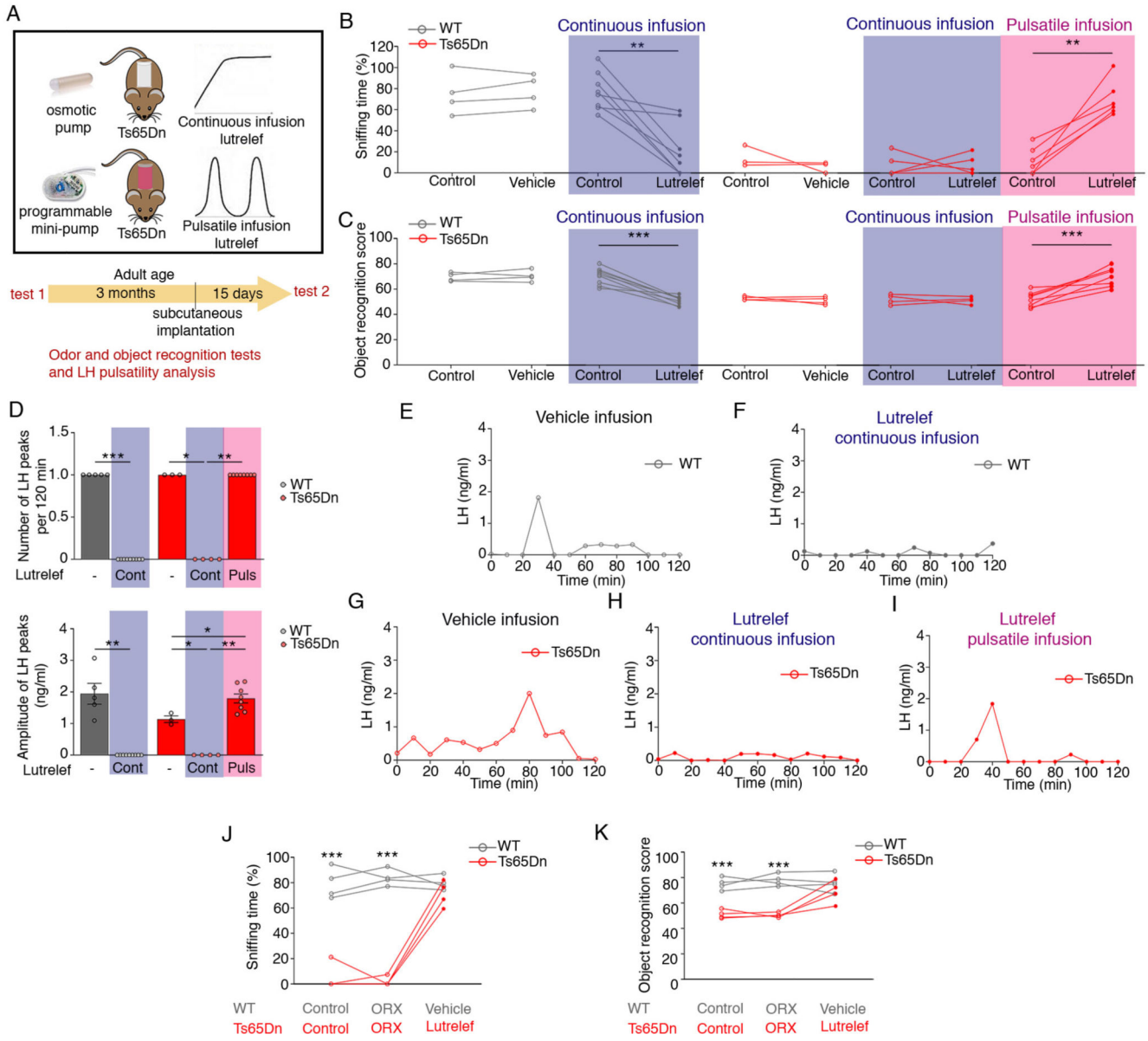

Fig. 6. Olfactory, cognitive deficit reversal requires GnRH pulsatility.

(**A**) Schematic of pharmacotherapy with Lutrelef, a clinically-used GnRH peptide, in adult Ts65Dn mice. Mice were implanted with osmotic pumps to receive a continuous infusion of vehicle or Lutrelef (0.25 μg/3h over 2 weeks), or with a programmable mini-pump (iPRECIO), to receive pulsatile Lutrelef infusion (0.25 μg/10 min every 3 hours over 2 weeks). (**B-I**) Effect of treatments on odor discrimination (**B**; n=4,8,3,5,6 mice), object recognition (C; n=4,9,4,4,8 mice) and LH pulsatility (**D-I**) (**D**: n=4,9,3,4,8 mice; each dot represents one subject). (**J-K**) Effects of Lutrelef in orchidectomized (ORX) mice (n=4). Values represent means ± SEM. * P<0.05,** P<0. 01,***P<0.001; paired Student's t-test or Wilcoxon matched-pair test (**B**,**C**), unpaired Student's t-test or Mann-Whitney U-test (**D**) or a two-way repeated-measures ANOVA followed by Sidak's post hoc test (**J**,**K**).

Europe PMC Funders Author Manuscripts

Europe PMC Funders Author Manuscripts

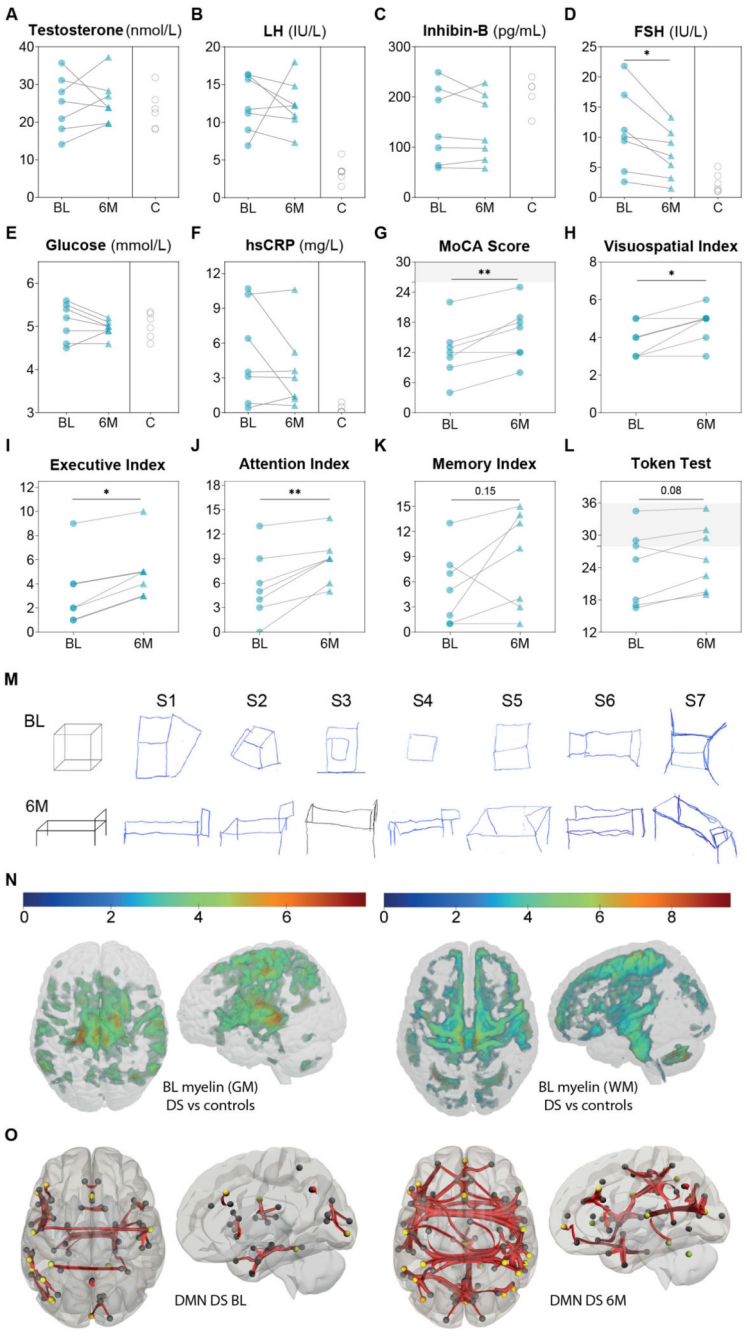

Fig. 7. Pulsatile GnRH improves patient brain connectivity, cognition.

(**A-F**) Biochemical profile at baseline (BL, blue dots, n=7) and after 6-month pulsatile GnRH therapy (6M, blue triangles, n=7), compared to healthy age- and sex-matched controls (C, open circles, n=5 for inhibin-B and n=6 for all the other parameters). (**G-L**) Results of cognitive tests in male Down syndrome patients (n=7) at BL (blue dots) and after 6M of GnRH therapy (blue triangles): MoCA total score, visuo-spatial index, executive index, attention index, memory index and Token test score. (**M**) 3D-drawings representing a cube and a bed, part of visuospatial index score of the MoCA at BL and 6M for each

subject (S1-S7). S2, S3, S5 and S7 improved at 6M. (**N**) Statistical parametric maps of brain anatomy differences between DS patients (n=8) and age-matched male controls (n=44) after $p_{FWE}<0.05$ correction for multiple comparisons at the whole-brain level. Voxel-based quantification of magnetization transfer (MT) saturation maps reveal volume loss in the cerebellum, anterior cingulate cortex, supplementary motor cortex, substantia nigra, thalamus, insula and primary motor cortex M1, and loss of myelin content in the thalamus, primary sensorimotor cortex S1/M1, angular gyrus, insula, and superior frontal and temporal gyri bilaterally. (**O**) Resting-state functional MRI comparison of functional connectivity in DS (n=7) at BL and after 6MGnRH therapy in the visual (including all occipital regions, the lingual gyrus and the cuneus) and sensorimotor (pre- and post-central gyri, middle frontal gyrus) default-mode network (DMN), connected to the superior parietal lobule, the superior temporal gyrus, some prefrontal areas and part of the anterior DMN (increased; FDR-corrected $p<0.0005$); as well as within the hippocampal regions of the ventral DMN linked to the amygdala (reduced; FDR-corrected $p<0.0005$). *$p<0.05$, **$p<0.01$. MoCA: Montreal cognitive assessment; FDR: false discovery rate; FWE: family-wise error; GM: grey matter; WM: white matter.

Europe PMC Funders Author Manuscripts